THE UNIVERSITY of EDINBURGH

Edinburgh Research Explorer

Clinical quantitative coronary artery stenosis and coronary atherosclerosis imaging: a Consensus Statement from the Quantitative Cardiovascular Imaging Study Group

Citation for published version:
Mézquita, AJV, Biavati, F, Falk, V, Alkadhi, H, Hajhosseiny, R, Maurovich-Horvat, P, Manka, R, Kozerke, S, Stuber, M, Derlin, T, Channon, KM, Išgum, I, Coenen, A, Foellmer, B, Dey, D, Volleberg, RHJA, Meinel, FG, Dweck, MR, Piek, JJ, Van de Hoef, T, Landmesser, U, Guagliumi, G, Giannopoulos, AA, Botnar, RM, Khamis, R, Williams, MC, Newby, DE & Dewey, M 2023, 'Clinical quantitative coronary artery stenosis and coronary atherosclerosis imaging: a Consensus Statement from the Quantitative Cardiovascular Imaging Study Group', *Nature Reviews Cardiology*. https://doi.org/10.1038/s41569-023-00880-4

Digital Object Identifier (DOI):
10.1038/s41569-023-00880-4

Link:
Link to publication record in Edinburgh Research Explorer

Document Version:
Peer reviewed version

Published In:
Nature Reviews Cardiology

General rights
Copyright for the publications made accessible via the Edinburgh Research Explorer is retained by the author(s) and / or other copyright owners and it is a condition of accessing these publications that users recognise and abide by the legal requirements associated with these rights.

Take down policy
The University of Edinburgh has made every reasonable effort to ensure that Edinburgh Research Explorer content complies with UK legislation. If you believe that the public display of this file breaches copyright please contact openaccess@ed.ac.uk providing details, and we will remove access to the work immediately and investigate your claim.

OPEN ACCESS

Download date: 09. Jun. 2023

CONSENSUS STATEMENT

Clinical quantitative coronary artery stenosis and coronary atherosclerosis imaging

Authors:

*Aldo J Vázquez Mézquita[1], *Federico Biavati[1],Volkmar Falk[2], Hatem Alkadhi[3], Reza Hajhosseiny[4,5], Pál Maurovich-Horvat[6], Robert Manka[7], Sebastian Kozerke[8], Matthias Stuber[9], Thorsten Derlin[10], Keith M Channon[11], Ivana Išgum[12], Adriaan Coenen[13], Bernhard Föllmer[1], Damini Dey[14], Rick Volleberg[15], Felix G Meinel[16], Marc R Dweck[17], Jan J. Piek[18],Tim van de Hoef[19],Ulf Landmesser[20], Giulio Guagliumi[21], Andreas A. Giannopoulos[22], René M Botnar[4,23], Ramzi Khamis[5], Michelle Claire Williams[17], †David E Newby[17], †Marc Dewey (editor request: ORCID: https://orcid.org/0000-0002-4402-2733)[1,24] on behalf of the Quantitative Cardiovascular Imaging Study Group

*A.J.V.M. and F.B. contributed equally as first authors

† D.N. and M.D. contributed equally as last authors

Correspondence to M.D., Charité – Universitätsmedizin Berlin, Charitéplatz 1, 10117 Berlin, Germany. dewey@charite.de

Author addresses:

1 Department of Radiology, Charité – Universitätsmedizin Berlin, Charitéplatz 1, 10117 Berlin, Germany

2 Department of Cardiothoracic and Vascular Surgery, Deutsches Herzzentrum der Charité (DHZC), Charité – Universitätsmedizin Berlin, DZHK (German Centre for Cardiovascular Research), Partner Site Berlin, Berlin, Germany and Department of Health Science and Technology, ETH Zurich, Switzerland

3 Diagnostic and Interventional Radiology, University Hospital Zurich, University of Zurich, Zurich, Switzerland

4 School of Biomedical Engineering and Imaging Sciences, King's College London, London, United Kingdom

5, National Heart and Lung Institute, Imperial College London, London, United Kingdom

6 Department of Radiology, Medical Imaging Center, Semmelweis University, Budapest, Hungary

7 Diagnostic and Interventional Radiology and Department of Cardiology, University Heart Center, University Hospital Zurich, University of Zurich, Zurich, Switzerland

8 Institute for Biomedical Engineering, ETH Zurich and University Zurich, Zurich, Switzerland

9 Department of Radiology, Centre Hospitalier Universitaire Vaudois (CHUV), Lausanne, Switzerland

10 Department of Nuclear Medicine, Hannover Medical School, Hannover, Germany

11 Radcliffe Department of Medicine, University of Oxford and Oxford University Hospitals, Oxford, United Kingdom

12 Department of Biomedical Engineering and Physics and Department of Radiology and Nuclear Medicine. Amsterdam UMC, University of Amsterdam, Amsterdam, the Netherlands

13 Department of Radiology, Erasmus University, Rotterdam, the Netherlands

14 Department of Imaging, Medicine, and Biomedical Sciences, Cedars-Sinai Medical Center, Los Angeles, California, USA

15 Department of Cardiology, Radboud University Medical Center, Nijmegen, the Netherlands

16 Department of Radiology, University Medical Centre Rostock, Rostock, Germany
17 Centre for Cardiovascular Science, University of Edinburgh, Edinburgh, United Kingdom
18 Amsterdam UMC, University of Amsterdam, Heart Center, Department of Clinical and Experimental Cardiology and Cardiovascular Sciences, Amsterdam, the Netherlands
19 Department of Cardiology, University Medical Center Utrecht, the Netherlands.
20 Cardiology Department, Deutsches Herzzentrum der Charité (DHZC), Charité – Universitätsmedizin Berlin, Berlin, Germany and , DZHK (German Centre for Cardiovascular Research), Partner Site, Berlin, Germany
21 Division of Cardiology, IRCCS Galeazzi Sant'Ambrogio Hospital, Milan, Italy
22 Department of Nuclear Medicine, Cardiac Imaging, University Hospital Zurich, University of Zurich, Zurich, Switzerland
23 Institute for Biological and Medical Engineering, Pontificia Universidad Católica de Chile, and Millennium Institute for Intelligent Healthcare Engineering, Santiago, Chile
24 Berlin Institute of Health at Charité, DZHK (German Centre for Cardiovascular Research), Partner Site, Berlin and Deutsches Herzzentrum der Charité (DHZC), Berlin, Germany

Abstract

Detecting and characterising coronary artery stenosis and atherosclerosis directly using imaging is key for clinical decision-making in patients with known or suspected coronary artery disease. Better imaging-based quantification can be achieved through technical improvements. Clinical consensus recommendations on the appropriateness of each imaging technique for direct coronary artery visualisation were derived in a three-step real-time Delphi process planned around the 2nd International Quantitative Cardiovascular Imaging (QCI) Meeting in September 2022. CT is the method of choice to rule out obstructive stenosis in patients with intermediate pre-test probability of coronary artery disease and enables quantitative assessment of coronary plaque with respect to dimensions, composition, location, and related risk of future cardiovascular events. MRI allows visualisation of coronary plaque and can be used in experienced centres as a radiation-free second-line option for non-invasive coronary angiography instead of CT. PET has greatest potential for quantifying inflammation within coronary artery plaque, while SPECT currently has a limited role in clinical coronary artery stenosis and atherosclerosis imaging. ICA is the reference standard for stenosis assessment but cannot characterise coronary plaques. IVUS and OCT are key invasive modalities for identifying plaques at higher risk of rupture. In this Consensus Statement, we provide Delphi-based clinical consensus recommendations on the preferred use of each imaging technique in specific patient populations and an outlook into the future technological potential.

Funded by the German Research Foundation (DFG, DE 1361/22-1).

Introduction

Because quantitative imaging of coronary atherosclerosis and stenosis has become widely available, interdisciplinary consensus about its role in clinical practice for the management of patients with suspected or known coronary artery disease (CAD) is highly desirable. During the 2nd Quantitative Cardiovascular Imaging (QCI) Meeting on September 9th, 2022, its present status and future potential were discussed from the viewpoint of clinicians (cardiologists, radiologists, and a cardiac surgeon), biomedical engineers, and computer scientists. This multidisciplinary approach was the basis for this Consensus Statement on the clinical appropriateness of quantitative coronary artery stenosis and atherosclerosis imaging.

Clinical need for coronary artery stenosis and atherosclerosis imaging

Appropriate assessment of the severity of coronary artery stenoses and the extent of the atherosclerotic burden is paramount for the selection of preventive measures and for guiding clinical decision-making in patients with known or suspected CAD. From a clinical perspective, three major questions need to be answered: 1) What is the best imaging technique for direct confirmation of CAD? 2) How can imaging help identify the best treatment strategy? 3) How can imaging improve procedural planning?

1) What is the best imaging technique for direct confirmation of CAD? Imaging has a crucial role in the diagnosis of obstructive CAD. While invasive coronary angiography (ICA) was the standard for a long time, several trials have since analysed the comparative effectiveness of ICA and computed tomography (CT) in stable chest pain[1–5] and have found no difference in diagnostic performance between CT and ICA for the identification of obstructive CAD. In patients with stable chest pain and an intermediate pre-test probability of CAD, the DISCHARGE trial showed a lower rate of major procedure-related complications during patient treatment when CT was used as the initial imaging test instead of ICA to define subsequent management[4,5]. In intermediate-risk patients with suspected acute coronary syndrome, the RAPID-CTCA trial showed no improvement of clinical outcomes at one year with early CT in addition to standard of care[6]. In contrast to CT, the role of other imaging modalities for direct visualisation of coronary stenosis has so far only been investigated in diagnostic studies[7], and randomised trials are lacking.

2) How can imaging help identify the best treatment strategy? Ideally, imaging would help to stratify patients who benefit from optimal medical treatment (OMT) and risk factor modification alone or from the addition of revascularisation by either percutaneous coronary intervention[8] (PCI) or coronary artery bypass

grafting (CABG). In patients with obstructive CAD and moderate/severe ischaemia, the ISCHEMIA trial showed that invasive treatment (predominantly PCI), compared to OMT and risk factor modification, did not prevent major adverse cardiovascular events until a median of 3.2 years of follow-up[9], highlighting the challenge of identifying patients who will benefit from revascularisation. A large meta-analysis found a lower risk of cardiac death especially among patients with multivessel chronic CAD undergoing revascularisation compared to OMT alone[10]. Multiple trials and an individual-patient-data meta-analysis of five trials that compared PCI vs CABG as the primary revascularisation therapy in patients with multivessel disease showed a survival benefit with CABG and a reduction in spontaneous myocardial infarction (MI)[11,12], which may be due to the different mode of revascularisation, namely CABG, which protects distal vascular territories (**FIG. 1**).

In addition, a network meta-analysis[13] underscored the importance of OMT. It showed that, in CAD patients without left main disease or reduced ejection fraction only, CABG was associated with a reduction of infarction and all-cause death compared to OMT alone (HR 0.58, 95% CI 0.48–0.70), but this was associated with a higher risk of stroke.

Because CABG is most beneficial in patients with more severe CAD, clinical quantitative coronary imaging for the assessment of the atherosclerotic plaque burden is highly desirable. The original SYNTAX score was found to allow selection of the best revascularisation therapy for individual patients based on the anatomical distribution, complexity, and severity of stenoses on ICA[14]. To overcome the shortcomings of purely anatomic scoring, comorbidities and other risk modifiers were included in SYNTAX II[15]. In retrospective analyses but not in prospective trials, the SYNTAX II and SYNTAX II 2020 successfully stratified patients benefiting from CABG vs PCI[16,17]. It would therefore be pivotal to test if the combination of clinical quantitative imaging with risk stratification could help to optimise treatment to prevent myocardial infarction, which is most commonly caused by rupture of plaques without previous flow limitations[18–20]. In addition to CT, there are two invasive imaging techniques that can identify high-risk plaque features: intravascular ultrasound (IVUS) and optical coherence tomography (OCT)[21]. In the PROSPECT study[22], it was estimated that a plaque burden >70% measured by IVUS was associated with major adverse cardiovascular events (MACE) during a follow-up of 3 to 4 years. However, it remains to be shown that these are actionable imaging findings that could help prevent events. One aspect is that only positron emission tomography (PET), and to some extent also magnetic resonance imaging (MRI), allows the identification and detection of coronary artery plaque inflammation, which is also linked to plaque rupture and subsequent MI and may thus trigger intensified OMT as an important target of coronary atherosclerosis imaging[23,24] (**FIG. 2**).

3) How can imaging improve procedural planning? Several trials have demonstrated that 'complete revascularisation', which was mostly determined by non-quantitative visual estimation of coronary stenoses in epicardial vessels, improves patient outcomes[25]. Fractional flow-reserve (FFR) can be used to guide appropriate use of PCI was introduced to limit the number of stents. The FAME-3 trial used this strategy in comparison to CABG in patients with multivessel disease with disappointing results. After one year, non-inferiority was not met for the primary endpoint (death, MI, cerebrovascular accident, or repeat revascularisation)[26]. This finding gives rise to two important considerations. First, the optimal target lesion for PCI remains to be determined. It may be a flow-limiting stenosis or a vulnerable plaque. Second, the revascularisation concept of CABG, which is fundamentally different from that of PCI and effectively provides the heart with a new autologous network of collaterals, may be particularly beneficial for preventing future MI in patients with a high plaque burden and multiple vulnerable plaques (**FIG. 1**). It is therefore of great importance to extract quantitative information from coronary atherosclerosis imaging pertaining to geometry, stability, and inflammatory status as well as total plaque burden[27]. Ultimately, this information may modify not only the mode but also the technique of revascularisation[24,28].

In this Consensus Statement, we present the current status of clinical quantitative imaging techniques for direct visualisation of coronary artery stenosis and atherosclerosis for detection of CAD, selection of the best treatment strategy, and improvement of procedural planning.

Methods of consensus

The latest advances in coronary artery stenosis and atherosclerosis imaging require experts in different fields to identify appropriate clinical applications. The complexity of the different imaging modalities means that a comprehensive consensus is needed. We used the Delphi method[29,30], asking participants a set of 29 questions (**Supplementary TABLE 1**) in a total of 3 rounds. We assembled the QCI group of 31 experts from different fields including 1 cardiac surgeon, 10 radiologists, 9 cardiologists, 6 biomedical engineers and scientists, and 5 computer engineers. The experts' talks were held during the 2nd QCI Consensus Meeting at Charité – Universitätsmedizin Berlin on September 9th, 2022, and in tandems from the clinical and frontier research perspective.

The first Delphi round took place online two weeks before the QCI meeting. The participants received a personalised link to the questionnaire via the Welphi web-application[31,32]. The second round took place on-site during the meeting, after the experts' talks. The third and final round took place again

online three weeks after the meeting. While answering each question, each participant was shown his/her answers from the previous round in the online tool and could revise this default answer when deemed appropriate (**Supplementary FIG. 1** and **2**). Additionally, before the second and third round, anonymised interim results from all experts in the previous round were shown in tabular format presenting the median for each question (**Supplementary TABLE 1** and **Supplementary File 1**). A total of 29 questions were presented in five categories: general clinical characteristics of coronary artery stenosis and atherosclerosis imaging modalities (5 questions), specific indications (8 questions), specific groups of patients (7 questions), specific coronary stenosis pathophysiology (3 questions), and specific atherosclerosis pathophysiology (6 questions) (**Supplementary TABLE 1**). The answers were entered using a Likert scale from 1 to 9, where 1 to 3 meant inappropriate, 4 to 6 meant uncertain, and 7 to 9 meant appropriate[33].The process was designed to present and weigh the advantages and disadvantages of each modality regarding different technical aspects and specific clinical indications. In this way, individual participants' opinions influenced each other towards a collective understanding of the subject discussed, and a consensus was reached in a streamlined and consistent manner (**FIG. 3**).

Technical characteristics, risk assessment, and challenges

Technical characteristics and challenges as well as advantages and disadvantages of the imaging modalities are summarised in **TABLE 1**.

Non-invasive imaging modalities for coronary stenosis and atherosclerosis assessment.

CT has high spatial and temporal resolution for noninvasive assessment of coronary stenosis and plaque composition[34,35] (**TABLE 1, FIG. 4** and **5**) within a single heartbeat using a low-dose protocol (3-5 mSv)[36–38]. On the other hand, CT requires intravenous administration of a highly concentrated iodine-based contrast agents and is susceptible to artefacts from high heart rates or coronary calcium[39] (**FIG. 2**, **TABLE 1**). It is important to note that intravenous contrast agents used for coronary CT angiography are associated with a lower rate of contrast-associated acute kidney injury (5.6%) compared with intra-arterial contrast agent administration for ICA (13.2%)[40]. Interestingly, physiological serum creatinine variation meeting the definition of acute kidney injury was similar to the rate of acute kidney injury 2 days after CT angiography[41] (**TABLE 1**). Major procedural complications of CT are rare and were reported in only 0.05% of patients, whereas the rate of major procedural complications of ICA without PCI was 1.0% and that of ICA with PCI was 5.6% in the DISCHARGE trial (**TABLE 1**). Major procedure-related complications were lower

by a factor of 4 in the CT-first group compared with the direct-to-ICA group in the DISCHARGE trial even including complications during the initial patient management following these diagnostic procedures[4]. This suggests that in terms of risk assessment, noninvasive CT coronary angiography is largely advantageous compared with directly proceeding to ICA. In expert centres, coronary MRI techniques offer the option of a free-breathing examination without ionising radiation, but cannot assess smaller vessels[23,42,43] and are only available for research settings at present [23,42]. Available sequences on most MRI scanners can assess stenotic segments, plaque inflammation and acute thrombi, and are not affected by artefacts produced by high-density calcium[44–48] **(TABLE 1, FIG. 4, FIG. 6**). On the other hand, cardiac MRI is limited by long acquisition times and lower spatial resolution in protocols designed for motion correction[39]. Importantly, claustrophobia occurs commonly during MRI with rates of 2% in outpatients and 10% in inpatients and MRI safety risks may arise from the referral of patients with absolute contra-indications (e.g. shrapnels) occurring at a rate of 0.4% (**TABLE 1**). PET and single-photon emission computed tomography (SPECT) are hybrid imaging modalities that in combination with CT provide the option of direct coronary imaging[49]. PET using 18F-sodium fluoride (NaF) can assess microcalcifications, while 68-galium (Ga)-DOTATATE visualises plaque inflammation, and 18F-glycoprotein 1 (18F-GP1) allows assessment of thrombus [49,50] (**TABLE 1, FIG. 7**). The rate of radiopharmaceutical adverse events is between 2.1 to 3.1 per 100,000 administrations (including cutaneous (rash, flush) and cardiovascular (e.g., hypotension, anaphylactoid) reactions)[51,52]. Effective radiation dose of PET/CT is approximately 10 mSv for the combination of coronary CT angiography, attenuation-correction CT and the radiotracer[24] (**TABLE 1)**. The use of PET/MRI can reduce effective dose to 4-5 mSv and wide field of view scanners may reduce this even further to ultra-low dose examinations. The assessment of small coronary vessels by PET alone is degraded because of its low spatial resolution (~ 4 mm), registration issues between PET and CT acquisitions, and motion artefacts[53,54]. SPECT is predominantly used for myocardial ischaemia imaging[33] and has a limited role in coronary plaque imaging in animal models[55].

Invasive imaging modalities for coronary stenosis and atherosclerosis assessment. With its high temporal and spatial resolution, ICA is the reference standard for stenosis assessment[56] (**FIG. 4**). ICA is invasive in nature, uses iodine contrast agents, and ionising radiation[56](**TABLE 1, FIG. 4**). As noted above, the intraarterial administration of contrast media for ICA resulted in a higher rate of contrast-associated acute kidney injury than intravenous contrast for CT in the randomised CAD-Man study[40] (**TABLE 1**). The rate of major procedural complications of ICA without PCI is approximately twenty times higher compared with CT (1.0% versus 0.05%)[4]. An important technical challenge of ICA is that vessel lumen dimensions

can be misrepresented because of foreshortening and tortuosity[56]. IVUS uses intra-coronary ultrasound and has a lower spatial resolution but a higher penetration than OCT, allowing the assessment of plaque affecting all the layers of the vessel wall as well as plaque composition[57–59] (**TABLE 1, FIG. 4**). OCT uses near-infrared light with a high temporal and spatial resolution (**TABLE 1, FIG. 4**). However, it has a lower penetration depth that limits the evaluation of coronary plaque to 500 µm within the luminal surface[59,60]. Both invasive intravascular modalities are limited by their rigid probes in tortuous, stenotic, highly calcified, and small vessels[61]. They have a role in the detection of clinically relevant stenoses and culprit lesions and in determining whether a plaque is at high risk of triggering future MACE[62]. With regards to risk assessment, coronary vasospasm is the most common major procedural complication of IVUS and OCT (approximately 3%) and pretreatment with nitrates is recommended. Additional major procedure-related complications (dissection, vessel occlusion, embo-lism) of both IVUS and OCT are rare (0.4%) but it is important to note that both entail the risks of ICA plus the additional IVUS- and OCT- procedure-related risks (**TABLE 1**).

Imaging modalities for stenosis assessment

The results for appropriateness regarding general characteristics, specific indications, specific groups of patients, and specific stenosis features are summarised in **FIG. 3** and **Supplementary File 1**.

Role in the assessment of stenosis. Meta-analyses demonstrated an excellent sensitivity of 100% of CT angiography for the diagnosis of obstructive coronary artery stenoses compared to ICA[63,64]. New-generation coronary MRI approaches have yielded an image quality comparable to that of CT in selected patients[65,66]. While MRI is a promising modality, large multi-centre studies comparing its diagnostic accuracy with ICA or CT are currently not available. PET allows to detect increased coronary plaque metabolism[67] (**TABLE 1**) but similar to SPECT does not allow clinical assessment of coronary stenosis (**FIG. 3**). Historically, ICA was considered the backbone of stenosis severity assessment and still has a role in identifying lesions that require immediate revascularisation (stenosis >90 %)[68]. IVUS and OCT impose an additional risk compared to ICA alone (**TABLE 1**) and are appropriate imaging modalities for patients with acute coronary syndrome and ST elevation while their general cost-effectiveness is uncertain[69,70] (**FIG. 3**).

Quantitative assessment of stenosis. CT is appropriate for stenosis measurement, e.g., of the minimum lumen diameter (MLD) and the minimum lumen area (MLA) with MLA being a better measure of luminal

narrowing in non-circular stenosis[71] (**FIG. 4**). It is also appropriate for females, young patients, and individuals with a high BMI (>30 kg/m^2) (**FIG. 3**). Coronary MRI is a potential option in expert centres for female and young patients with an accuracy of 79% for the detection of obstructive CAD compared with ICA; however, MRI is not recommended for coronary stenosis measurement because of low spatial resolution and susceptibility to artefacts[23] (**TABLE 1, FIG. 3**). Due to the lack of studies evaluating the accuracy of the CT component of PET and SPECT, both imaging modalities are currently considered inappropriate for stenosis quantification (**FIG. 3**).

ICA has a high accuracy in measuring stenosis but interobserver variability is substantial[72] and can be improved through the use of quantitative coronary angiography (QCA)[73], while ICA is preferable over CT in patients with high heart rates (**TABLE 1, FIG. 3**). Stenosis quantification by IVUS and OCT can be performed with absolute (e.g., MLA) and relative measures (e.g., percentage area stenosis) (**FIG. 4**) and both invasive modalities are appropriate for stenosis measurement with low susceptibility to artefacts while the size of the probes prevents the assessment of distal and very stenotic segments (**TABLE 1)**. Although generally larger than measured on ICA[74], the average luminal diameter measured by IVUS, and especially OCT, corresponds well with actual dimensions in phantom models (measured diameter between -2.9% and 8.0%), and the measurements are highly reproducible[74,75].

Indications and clinical applications. CT is most appropriate for assessing coronary anatomy and in stable chest pain patients with low to intermediate pre-test probability and is the preferred choice after heart transplantation[4,76,77] (**FIG. 3**). The clinical indications for coronary MRI are currently uncertain because of a lack of randomised trials[78]. The high negative predictive value in expert centres makes coronary MRI a possible non-invasive second-line option for direct coronary assessment in patients with low to intermediate pre-test probability[78] while the appropriateness of PET and SPECT remain generally uncertain (**FIG. 3**).

The DISCHARGE trial[4] and smaller randomised trials[5] found several benefits for a treatment strategy guided by CT instead of ICA in stable chest pain patients with intermediate pre-test probability of disease and thus, ICA remains the most appropriate imaging modality for direct coronary assessment in patients with high pre-test probability. In acute coronary syndrome, ICA is most appropriate, and the additional use of IVUS or OCT is considered appropriate if ST elevation is present(**FIG. 3**). However, a meta-analysis has revealed only moderate accuracy compared with FFR for different MLA cut-off values proposed for identification of hemodynamically significant stenosis by IVUS and OCT[79,80].

Future developments. Improvements of in-plane spatial resolution of CT to 0.16-0.25 mm[81] will reduce blooming artefacts for more accurate stenosis quantification and improved lumen visualisation in the presence of coronary stent struts[82]. In MRI, automated trigger delay determination, scan planning, and image reconstruction will enable adequate spatial resolution within a single breath-hold[83]. Automated calibration and lumen contouring in ICA may further ease and increase the use of QCA for stenosis quantification. For IVUS and OCT, imaging-derived computational flow indices allow improved identification of hemodynamically significant stenoses compared to luminal measurements only[84,85] .

Key points for stenosis assessment

- CT is most appropriate as an initial test for diagnosing CAD in patients with stable chest pain and low to intermediate clinical likelihood of obstructive CAD.
- Not using ionising radiation, coronary MRI can become a second-line option for direct coronary assessment in patients with low to intermediate pre-test probability.
- ICA is the most appropriate test in patients with high pre-test probability and acute coronary syndrome.
- PET and SPECT have no role in the direct assessment of stenosis severity.
- IVUS and OCT are preferred in acute coronary syndrome with ST elevation and for planning stent placement.

CT for coronary atherosclerosis imaging

Role in the assessment of atherosclerosis. CT provides qualitative and quantitative information on the total coronary plaque burden and composition (**FIG. 3**, **Supplementary File 1**). Specifically, CT allows detection and quantification of calcified, non-calcified, and partially calcified plaque (**FIG. 2**). Moreover, analysis of plaque characteristics in CT has been shown to allow identification of high-risk plaque features[86,87] (**FIG. 5**).

Quantitative assessment of atherosclerosis. Coronary artery calcium (CAC) plaque burden is quantified using the Agatston, volume, or mass CAC scores[88,89]. The CAC score is a strong and independent predictor of cardiovascular events[90,91] and, therefore, is recommended to refine the 10-year risk stratification[92]. Low-attenuation plaque burden (< 30 Hounsfield units) > 4% on CT was shown to be associated with fatal and nonfatal MI in patients with stable chest pain in the SCOT-HEART trial (HR: 4.65; 95% CI, 2.06–10.5;

P<0.001)[93]. Plaque morphology on CT provides further valuable prognostic information[94]. High-risk coronary plaque features on CT, in addition to a CAC score of 400 or more[4,95], include low attenuation, positive remodelling, napkin-ring sign and spotty calcifications[86,87] (**FIG. 5**).

Indications and clinical applications. CT is most appropriate for quantifying total coronary plaque burden and appropriate to assess coronary plaque morphology and composition. The detection of culprit plaque is appropriate using CT, yet was rated higher using IVUS and OCT[96] (**FIG. 3**). In asymptomatic individuals at an intermediate risk of CAD, CAC scoring, based on non-contrast CT, adds prognostic value beyond clinical risk factors and can guide decision-making regarding risk factor modification[95]. Coronary plaque on CT is visually intuitive and can be directly explained to patients and, therefore, may improve adherence to medical therapy well as lead to more statin therapy recommendations[97]. Analysis of the pericoronary adipose tissue (PCAT) surrounding the coronary arteries on CT has emerged as a new approach to detecting and quantifying coronary artery inflammation[98] by detecting a higher attenuation as an indirect biomarker of molecular and cellular changes[96] (**FIG. 5**).

Future development. New software will allow rapid, fully automated whole coronary tree plaque quantification and characterisation and may ultimately be used as a support tool for routine clinical decision-making [99]. In addition, further research on PCAT will provide more insights into its possible clinical utility[100,101].

Key points for CT

- CT's spatial resolution enables quantitative assessment of coronary plaque with respect to dimensions, composition, location, and related risk of future cardiovascular events while it is the most appropriate modality for quantification of the total coronary plaque burden (**FIG. 3**).
- Higher and/or irregular heart rates, extensive coronary calcifications, and coronary stents hinder the evaluation of coronary atherosclerosis (**TABLE 1**).
- Automated whole-tree coronary plaque software, together with higher temporal and spatial resolution provided by new CT scanners, will facilitate quantification of coronary atherosclerosis.

MRI for coronary atherosclerosis imaging

Role in the assessment of atherosclerosis. Black-blood imaging sequences[102](**FIG. 6**) are used to assess the lumen and vessel wall and detect wall thickening as a marker of positive remodelling[103–106]. Dark-blood

T1-weighted imaging detects hallmarks of plaque haemorrhage and luminal thrombi as hyperintense signals, which indicate the formation of methaemoglobin 12 to 72 hours following a haemorrhagic event[107](**FIG. 6**, **Supplementary File 1**). Finally, intra-plaque inflammation (**FIG. 2**), and extracellular expansion related to angiogenesis have been targeted using contrast-enhanced T1-weighted imaging after administration of a gadolinium-based contrast agent, and results demonstrate a correlation of dynamic and late signal enhancement with the severity of atherosclerosis[108] (**FIG. 6**).

Quantitative assessment of atherosclerosis. High signal intensity of coronary plaque on noncontrast MRI, which correlates with a higher likelihood of unstable plaque[109], can be quantified on T1-weighted inversion-recovery images Intriguingly, the extent of high-intensity plaque was found to decrease after statin therapy[110]. Sato et al.[111] have shown that the predominant substrate for such high-intensity plaque in stable CAD is intraplaque haemorrhage and not lipids, which is in agreement with findings of near-infrared spectroscopy IVUS (NIRS-IVUS) and indicates how MRI may contribute to the guidance and monitoring of therapy.

Indications and clinical applications. The clinical use of MRI is considered uncertain, mostly because of its limited resolution and 3D coverage (**FIG. 3**). Black- and dark-blood MRI may become alternatives to CT for the non-invasive assessment of coronary atherosclerosis[112]. Imaging high-risk plaque features may help to better stratify patients' risk and thus improve tailoring of medical therapy.

Future development. Spatial resolution will be enhanced by three-dimensional (3D) imaging with isotropic voxel sizes between 0.8 and 1.5 mm and acquisition times of 10 to 15 min[39,46]. Signal may be boosted by administering targeted gadolinium- or iron-based contrast agents[113]. Alternatively, fluorine-based imaging agents may improve contrast given the absence of background signal[114]. Additional efforts to boost resolution include non-rigid motion correction for signal acquisition during extended periods of the cardiac cycle[115].

Key points for MRI

- MRI allows visualisation of wall thickness, intraplaque haemorrhage, and luminal thrombi as high-risk coronary plaque features but is limited by motion artefacts.
- MRI is currently not appropriate for use in clinical practice because it has too low a resolution and lacks 3D coverage in comparison to CT (**TABLE 1**).

- New technology to improve spatial resolution, motion correction, as well as new contrast agents may make MRI a non-invasive alternative to CT.

PET for coronary atherosclerosis imaging

Role in the assessment of atherosclerosis. PET allows interrogation of disease activity within coronary plaque, and research has focused largely on the detection of coronary inflammation, calcification, and thrombosis[24,116,117] (**FIG. 2**). Radiotracers specifically targeting inflammation can be administered to identify and to characterise distinct phases of inflammation[118]. Examples include targeting of glucose metabolism in activated macrophages with ^{18}F-fluorodeoxyglucose[117], chemokine receptor CXCR4 expression on leukocytes and polarised macrophages[118] and somatostatin receptor subtype-2 expression in proinflammatory macrophages with ^{68}Ga-DOTATATE[119],and calcification activity using the radiotracer ^{18}F-sodium fluoride (NaF)[120] (**FIG. 7**).

Quantitative assessment of atherosclerosis. Most studies have been conducted with the radiotracer ^{18}F-NaF, which has been validated as a marker of calcification and disease activity using histology as standard of reference[24] (**FIG. 7**). Its uptake demonstrates a close association with disease progression and a change in CAC scores[121]. Importantly, baseline ^{18}F-NaF identifies culprit plaque, and total coronary microcalcification activity independently predicts subsequent fatal or non-fatal MI (hazard ratio 7.1, 95% confidence interval 2.2 to 25.1; p=0.003)[120].

Indications and clinical applications. PET is considered the most appropriate imaging modality for assessing coronary plaque inflammation (**FIG. 3**, **Supplementary File 1**) but remains primarily a research tool. ^{18}F-FDG PET is already used to monitor the pharmacologic modulation of inflammation in extra-coronary atherosclerotic plaque in clinical trials of novel anti-inflammatory drugs[122,123]. Moreover, PET has provided translationally relevant insights into plaque pathobiology and the relevance of systemic interactions for disease progression[116,124]. The prospective multicentre non-randomised international clinical PREFFIR study[125] recently confirmed the ability of ^{18}F-NaF PET to predict subsequent MI[120] and cardiovascular death in patients with advanced multivessel CAD and a history of recent MI. These findings can help identify patients with active disease states who may benefit from intensive medication (e.g., PCSK9 or IL1 inhibition).

Future development. New tracers will allow the more specific interrogation of coronary inflammation and other key processes such as fibrosis[126] and thrombus formation[127]. Advances in PET detector technologies will lead to better resolution and, thus, higher sensitivity[128]. Finally, image processing solutions to address motion can markedly enhance image quality and are becoming clinically available[129].

Key points for PET

- PET is considered most appropriate for quantifying coronary plaque inflammation, yet is susceptible to motion artefacts and has limited temporal and spatial resolution (**TABLE 1**) and therefore currently remains a research tool.
- Technical advances and software improvements will improve motion correction and overcome limited spatial and temporal resolution.
- ^{18}F-NaF PET of calcification activity predicts subsequent disease progression and event risk and has the potential to improve risk stratification and identification of patients who require a more intensive therapy.

ICA for coronary atherosclerosis imaging

Role in the assessment of atherosclerosis. ICA is the reference standard for the diagnosis of obstructive CAD[4] but has a limited role in the direct visualisation of coronary atherosclerosis (**FIG. 3**, **Supplementary File 1**).

Quantitative assessment of atherosclerosis. ICA detects the presence of atherosclerotic plaque based on the imprint left on the vessel contour and therefore provides limited information on plaque morphology and composition (**FIG. 3**). Nonetheless, deformation of the vessel wall by circumferential tensile stress from the pulsatile arterial pressure is directly dependent on tissue stiffness and therefore on the plaque composition (**FIG. 8**). This deformation of the coronary artery, termed radial wall strain (RWS), can be derived from ICA and presents another avenue for clinical application of advanced ICA technology[130] (**FIG. 8).**

Indications and clinical applications. ICA is appropriate for culprit coronary plaque detection (**FIG. 3**). As supported by our Delphi results, ICA is appropriate in patients with a high pre-test probability of CAD. Moreover, ICA is also indicated if a patient remains symptomatic despite guideline-directed medical treatment and in case of high-risk anatomy CAD[131] **(FIG. 3, Supplementary File 1**).

Future development. Promising ICA-based techniques to assess coronary atherosclerosis such as RWS must be further explored[130]. An additional ICA-based technique is determination of endothelial shear stress, which indicates coronary artery regions prone to developing plaques based on computational fluid dynamics, and thus, a potential parameter for risk stratification in patients with CAD[19,132].

Key points for ICA

- ICA is appropriate for the detection of culprit coronary plaque especially in patients with acute coronary syndrome, yet does not directly visualise the vessel wall and plaque composition.
- Coronary RWS is indirectly determined by coronary plaque composition and could potentially have a role clinically (**FIG. 8**).
- ICA is appropriate in patients with stable chest pain and a high pre-test probability of CAD (>60%).

IVUS for coronary atherosclerosis imaging

Role in the assessment of atherosclerosis. IVUS can characterise the morphology and composition of coronary artery plaque with a much higher penetration depth (4-8 mm) than OCT (0.4-2.0 mm)[70]; but with lower spatial resolution (**TABLE 1**). IVUS allows visualisation of all three layers of the coronary vessel wall and the detection of high-risk plaques that can reduce the effectiveness of PCI (**FIG. 9**).

Quantitative assessment of atherosclerosis. Positive remodelling is a common finding in early atherosclerosis that can be detected using IVUS and is associated with plaque rupture and thrombus formation[133] (**FIG. 2**). In the PROSPECT study[22], IVUS-based determination of a plaque burden larger than 70% in patients with acute coronary syndrome was associated with non-culprit MACE during a follow-up of 3 to 4 years (HR: 5.03, 95% CI: 2.51–10.11, p<0.001). IVUS probes integrating NIRS allow detection and quantification of lipid-rich plaques based on a maximum 4 mm lipid core burden index ≥400, which was found to help in identifying patients at higher risk for subsequent MACE (HR:3.39, 95% CI: 1·85–6·20, p<0·0001) in 24-month follow-up[134]. However, artefacts such as posterior shadowing in calcified plaque, reverberation, and non-uniform rotational distortion can degrade coronary plaque visualisation in IVUS[135] (**FIG. 9**).

Indications and clinical applications. IVUS is appropriate to assess coronary plaque composition and to detect culprit plaque (**FIG. 3**, **Supplementary File 1**). IVUS is considered less appropriate than CT for estimating total plaque burden and less appropriate than PET for assessing coronary plaque inflammation. It is also useful for identifying stent failure, particularly by determining malapposition, underexpansion, and edge dissection[62] (**FIG. 9**). The ULTIMATE trial demonstrated that the use of IVUS during the implantation of drug-eluting stents reduced the cardiovascular death rate compared to the use of ICA alone[136].

Future development. Current research focuses on automatic detection and measurement of coronary plaque during the procedure[137,138]. IVUS technologies that incorporate other imaging modalities (OCT/NIRS) and the estimation of FFR will enhance the identification of high-risk coronary plaques and their haemodynamic repercussion, respectively[62,70].

Key points for IVUS

- IVUS is appropriate for assessment of coronary plaque composition and detection of culprit coronary plaque.
- Assessing target vessels before stent implantation and detecting stent failure are important clinical applications of IVUS which will benefit from the development of automated detection and quantification of coronary plaque.

  Detection of superficial lesions with a high risk of rupture is an important area of IVUS research that can ultimately close the gap towards OCT.

OCT for coronary atherosclerosis imaging

Role in the assessment of atherosclerosis. OCT is an invasive imaging modality that provides real-time tomographic views of coronary plaque at very high resolution by using infrared light and fibreoptic technologies[62]. OCT has the highest spatial resolution to assess superficial coronary plaque lesions but lower penetration depth than IVUS[62], which also is its major limitation as it precludes assessment of the total coronary plaque burden. When used to assess suspected stent failure, OCT can detect uncovered struts, distinguish neoatherosclerosis from neointima, and identify thrombus and is more accurate in revealing stent underexpansion, malapposition, and edge dissection[139–141].(**FIG. 10**).

Quantitative assessment of atherosclerosis. OCT can differentiate the phenotype of culprit coronary plaque and to identify TCFA (i.e., cap < 65-70 μm)[60,142] (**FIG. 10)**. Moreover, OCT can measure the thickness of the fibrous cap[60], identify high-risk plaques[61,143] and macrophages (**FIG. 10**), and quantify plaque extension[144].

Indications and clinical applications. Because of its high spatial resolution, OCT is most appropriate for assessment of coronary plaque morphology and equally appropriate as IVUS for determination of coronary plaque composition and culprit coronary plaque detection (**FIG. 3**, **Supplementary File 1**). The detailed visualisation of luminal superficial lesions allows identification of underlying causes of MI with non-obstructive coronary arteries (MINOCA) such as spontaneous coronary artery dissection and embolic disease[61]. In the ILUMIEN III: OPTIMISE PCI trial, OCT-guided PCI was able to achieve higher stent expansion measured as minimum stent area compared with ICA-guided PCI, but was not superior to IVUS-guided PCI[145].

Future development. Automated identification and quantification of coronary plaques by OCT is a subject of current research[146,147]. A combination of OCT with other intravascular imaging modalities (IVUS/NIRS) and OCT-based FFR may be able to more comprehensively assess coronary plaque and flow impact after stent implantation[143,148,149]. This may facilitate better identification of plaques with a higher risk of complications.

Key points for OCT

- OCT has high spatial resolution and thus allows accurate assessment of superficial lesions while its penetration depth is lower than that of IVUS.
- The main challenges of OCT include its invasive nature, the expertise required in imaging interpretation, and its limited penetration depth.
- OCT is recommended for guiding and optimising stent placement, especially in patients with complex lesions and anatomy.

Conclusions

Several modalities are available for clinical quantitative coronary artery stenosis and atherosclerosis imaging. CT is accurate and reliable for stenosis assessment and quantification of total coronary plaque volume, making CT most appropriate for directing treatment in patients with stable chest pain and an

intermediate probability of CAD[27]. Even though MRI is currently not widely used in the clinical setting and is mostly used at expert centres, it has potential to become a reliable tool to assess stenosis and plaque morphology without ionising radiation exposure provided further technical improvements relevantly increase its robustness. PET has a role in the quantitative assessment of coronary plaque inflammation, making it a preferred modality for treatment monitoring. ICA is considered the reference standard for the evaluation of patients with stable chest pain and a high probability of coronary stenosis as well as for patients with acute coronary syndrome. IVUS and OCT are intravascular imaging modalities that play a relevant role both in the estimation of coronary stenosis severity and in plaque characterisation for treatment planning.

The clinical potential of these modalities can be substantially improved by technical advances. In CT, new technologies aim at improving spatial and temporal resolution as well as automated quantification and characterisation of coronary plaque. The spatial resolution of MRI will be enhanced by reduction of the voxel size and shorter acquisition times, and better signal enhancement will be achieved with new contrast agents. The role of PET will expand by the translation of research findings into clinical practice and the development of new tracers for the detection of plaque vulnerability. QCA will help in the standardisation of stenosis assessment by ICA, while RWS will contribute information derived from estimating the deformity of the vessel wall caused by coronary plaques. Anatomical measurements in IVUS and OCT will enable determination of coronary flow by the integration of FFR into the same catheters.

No single quantitative coronary imaging modality is best for all groups of patient or disease types and not all are equally available with similar local expertise at all clinical centres. Using a Delphi method, we determined which imaging modalities are better suited for specific patient groups (**FIG. 3)**. In conclusion, this clinical consensus statement shows the current advantages, disadvantages, and expected future development of different imaging modalities for clinical quantitative coronary artery stenosis and atherosclerosis imaging. This will help examiners to appropriately choose the best imaging modality based on the specific clinical scenario, individual patient characteristics, and the availability of each imaging modality.

Acknowledgment

We thank the German Research Foundation for funding the 2nd Quantitative Cardiovascular Imaging Meeting and Consensus Statement on quantitative assessment of coronary artery stenosis and atherosclerosis (DE 1361/22-1).

Author contributions

A.J.V.M. and F.B. wrote the first draft of the introduction and the technical characteristics and challenges sections, which was edited by M.D. before all authors reviewed and revised these sections. A.J.V.M. and F.B. wrote the first draft of the methods of consensus section, which was edited by M.D. before all authors reviewed and revised this section. V.F. and F.B. wrote the "Why do we need coronary imaging?" section. A.J.V.M. wrote the first draft of the "Technical characteristics and challenges" section including table 2, which were edited by A.C., A.G., M.C.W., D.D., D.E.N., R.V., G.G., B.F., and M.D. before all authors reviewed and revised this section. H.A., R.H., A.C., F.M., R.M.B., and R.K. wrote the first draft of the "Imaging modalities for stenosis assessment" section, which was edited by A.J.V.M., F.B. and M.D. before all authors reviewed and revised this section. Regarding the "Imaging modalities for atherosclerosis assessment" section, F.M., I.I., P.M. and K.M.C. wrote the first draft of the CT subsection ,which was edited by A.J.V.M, F.B. and M.D. before all authors reviewed and revised it; R.M., S.K. and M.S. wrote the first draft of the MRI subsection which was edited by A.J.V.M, R.M.B., R.K. and M.D. before all authors reviewed and revised it; D.E.N., M.R.D. and T.D. wrote the first draft of the PET subsection, which was edited by A.J.V.M. and M.D before all authors reviewed and revised it; J.P. and T.V.D.H. wrote the first draft of the ICA subsection, which was edited by A.J.V.M. and M.D. before all authors reviewed and revised it; U.L. and A.J.V.M. wrote the first draft of the IVUS subsection, which was edited by M.D. before all authors reviewed and revised it; G.G. wrote the first draft of the OCT subsection, which was edited by A.J.V.M., F.B. and M.D. before all authors reviewed and revised it. All authors contributed to researching data and discussion of content. All authors reviewed and edited the entire manuscript before submission.

Competing interests

A.J.V.M, F. B, B.F., R.H., R.V., T.D, S.K.,T.V.D.H., R.M.B., and R.K. declare no conflicts of interest. V.F. has received educational grants, fees for lectures and speeches, fees for professional consultation, as well as research and study funds from: Medtronic GmbH, Biotronik SE & Co, Abiomed GmbH, Abbott GmbH & Co. KG, Boston Scientific, Edwards Lifesciences, Berlin Heart, Novartis Pharma GmbH, JOTEC/CryoLife GmbH, LivaNova and Zurich Heart. H.A. has received institutional grants from Bayer, Guerbet, Canon and Siemens. He is currently part of the speaker's bureau of Siemens. A.C.'s spouse is employed by GE Healthcare. D.D. has received software royalties from Cedars-Sinai Medical Center and grant support from NIH/NHLBI. M.R.D. is supported by the British Heart Foundation (FS/SCRF/21/32010) and is the recipient of the Sir Jules Thorn Award for Biomedical Research 2015 (15/JTA). He also has received speaker fees from Pfizer, Edwards and Novartis. He has received consultancy fees from Novartis, Jupiter Bioventures, Beren and Silence therapeutics. He is the Director of Image Analysis Core Lab within the Edinburgh Clinical Research Facility, University of Edinburgh. F.G.M. has received a research grant from GE Healthcare and speaker honoraria from GE Healthcare, Circle Cardiovascular Imaging and Bayer Vital. I.I. has received institutional research grants by Pie Medical Imaging BV and Esaote S.p.A. She also received an institutional research grant funded by Dutch Technology Foundation with participation of Pie Medical Imaging BV and Philips Healthcare. Institutional research grants by Pie Medical Imaging BV and Esaote S.p.A.; Institutional research grant funded by Dutch Technology Foundation with participation of Pie Medical Imaging BV and Philips Healthcare; Co-inventor on patents (US 10,176,575 B2, US 10,395,366 B2, US 11,004,198 B2, US 10,699,407 B2) and patent applications (17317746, 16911323) on detection of functionally significant coronary stenosis. P.M.H. is a shareholder of Neumann Medical Ltd. K.M.C. is funded by the British Heart Foundation, and is a co-founder and shareholder in Caristo Diagnostics, a University of Oxford spin-out company involved in

medical imaging. A.G. has received grant support from Promedica Stiftung and the Iten-Kohaut Foundation in collaboration with the USZ Foundation and reports speaker honoraria from GE Healthcare. M.S. receives grant support from the Swiss National Science Foundation (SNSF) and non-monetary research support from Siemens Healthineers. R.M. has received speaker fees from Siemens and Bayer. J.P. is a consultant for Philips. G.G. has a consultant agreement with Abbott Vascular, Infraredx, Gentuity and Panovision. He has also received a research grant in the las 36 months by Abbott Vascular, Amgen, and Infraredx. M.C.W. has given talks for Canon Medical Systems, Siemens Healthineers and Novartis. M.C.W is supported by the British Heart Foundation (FS/ICRF/20/26002). U.L. has received research grants to institutions from Abbott and he is honorary advisory lecturer from Abbott and Boston Scientific. D.E.N. receives grants, acts as a consultant, and has clinical trial contracts with: Abbott, Amgen, AstraZeneca, Autoplaque, BMS, Boehringer Ingelheim, Elly Lilly, GE, GSK, Jansen, Life Molecular Imaging, MSD, Novartis, Pfizer, Phillips, Roche, Sanofi, Siemens, Silence, SOFIE, Toshiba, UCB, Vifor, Wyeth, Zealand. He collaborates with the publication's chair from the BMJ Group, and Elsevier. He has received research funding from: British Heart Foundation, Medical Research Council, Wellcome Trust, Chief Scientist Office, and Chest Heart Stroke Scotland. He is the chief Investigator of the SCOT-HEART and PRE18FFIR trials. M.D. has received grant support from the FP7 Program of the European Commission for the randomized multicenter DISCHARGE trial (EC-GA 603266 in HEALTH.2013.2.4.2-2). He also received grant support from German Research Foundation (DFG) in the Heisenberg Program (DE 1361/14-1, DFG project number: 213705389), graduate program on quantitative biomedical imaging (BIOQIC, GRK 2260/1, DFG project number: 289347353), for fractal analysis of myocardial perfusion (DE 1361/18-1, DFG project number: 392304398), the DFG Priority Programme Radiomics (DFG project number: 402688427) for the investigation of coronary plaque and coronary flow (DE 1361/19-1 [DFG project number: 428222922] and DE 1361/20-1 [DFG project number: 428223139] in SPP 2177/1), the GUIDE-IT project on data sharing of medical imaging trials (DE 1361/24-1 [DFG project number: 495697118]), the Quantitative Cardiovascular Imaging (QCI) meeting (DE 1361/22-1), and the Future of Medical Imaging meeting (DE 1361/28-1). He also received funding from the Berlin University Alliance (GC_SC_PC 27) and from the Digital Health Accelerator of the Berlin Institute of Health. M.D. is European Society of Radiology (ESR) Publications Chair (2022-2025); and the opinions expressed in this article are the author's own and do not represent the view of ESR. Per the guiding principles of ESR, the work as Publications Chair is on a voluntary basis and only remuneration of travel expenses occurs. M.D. is also the editor of Cardiac CT, published by Springer Nature, and offers hands-on courses on CT imaging (www.ct-kurs.de). Institutional master research agreements exist with Siemens, General Electric, Philips, and Canon. The terms of these arrangements are managed by the legal department of Charité – Universitätsmedizin Berlin. M.D. holds a joint approved patent with Florian Michallek on dynamic perfusion analysis using fractal analysis (EPO 2022 EP3350773A1, and USPTO 2021 10,991,109).

References

1. Dewey, M. *et al.* Evaluation of computed tomography in patients with atypical angina or chest pain clinically referred for invasive coronary angiography: randomised controlled trial. *BMJ* **355**, i5441 (2016).
2. Chang, H.-J. *et al.* Selective Referral Using CCTA Versus Direct Referral for Individuals Referred to Invasive Coronary Angiography for Suspected CAD: A Randomized, Controlled, Open-Label Trial. *JACC Cardiovasc Imaging* **12**, 1303–1312 (2019).
3. Rudziński, P. N. *et al.* Efficacy and safety of coronary computed tomography angiography in patients with a high clinical likelihood of obstructive coronary artery disease. *Kardiol Pol* **80**, 56–63 (2022).
4. DISCHARGE Trial Group *et al.* CT or Invasive Coronary Angiography in Stable Chest Pain. *N Engl J Med* **386**, 1591–1602 (2022).
5. Kheiri, B. *et al.* Computed Tomography vs Invasive Coronary Angiography in Patients With Suspected Coronary Artery Disease: A Meta-Analysis. *JACC Cardiovasc Imaging* **15**, 2147–2149 (2022).
6. Gray, A. J. *et al.* Early computed tomography coronary angiography in patients with suspected acute coronary syndrome: randomised controlled trial. *BMJ* **374**, n2106 (2021).
7. Schuetz, G. M., Zacharopoulou, N. M., Schlattmann, P. & Dewey, M. Meta-analysis: noninvasive coronary angiography using computed tomography versus magnetic resonance imaging. *Ann Intern Med* **152**, 167–77 (2010).
8. Perera, D. *et al.* Percutaneous Revascularization for Ischemic Left Ventricular Dysfunction. *New England Journal of Medicine* **387**, 1351–1360 (2022).
9. Maron, D. J. *et al.* Initial Invasive or Conservative Strategy for Stable Coronary Disease. *New England Journal of Medicine* **382**, 1395–1407 (2020).
10. Navarese, E. P. *et al.* Cardiac mortality in patients randomised to elective coronary revascularisation plus medical therapy or medical therapy alone: a systematic review and meta-analysis. *Eur Heart J* **42**, 4638–4651 (2021).
11. Gaudino, M. *et al.* Overall and Cause-Specific Mortality in Randomized Clinical Trials Comparing Percutaneous Interventions With Coronary Bypass Surgery: A Meta-analysis. *JAMA Intern Med* **180**, 1638–1646 (2020).
12. Head, S. J. *et al.* Mortality after coronary artery bypass grafting versus percutaneous coronary intervention with stenting for coronary artery disease: a pooled analysis of individual patient data. *Lancet* **391**, 939–948 (2018).
13. Galli, M. *et al.* Revascularization strategies versus optimal medical therapy in chronic coronary syndrome: A network meta-analysis. *Int J Cardiol* **370**, 58–64 (2023).
14. Serruys, P. W. *et al.* Percutaneous coronary intervention versus coronary-artery bypass grafting for severe coronary artery disease. *N Engl J Med* **360**, 961–72 (2009).
15. Farooq, V. *et al.* Anatomical and clinical characteristics to guide decision making between coronary artery bypass surgery and percutaneous coronary intervention for individual patients: development and validation of SYNTAX score II. *Lancet* **381**, 639–50 (2013).
16. Takahashi, K. *et al.* Redevelopment and validation of the SYNTAX score II to individualise decision making between percutaneous and surgical revascularisation in patients with complex coronary artery disease: secondary analysis of the multicentre randomised controlled SYNTAXES trial with external cohort validation. *Lancet* **396**, 1399–1412 (2020).
17. Hara, H. *et al.* External Validation of the SYNTAX Score II 2020. *J Am Coll Cardiol* **78**, 1227–1238 (2021).
18. Doenst, T. *et al.* PCI and CABG for Treating Stable Coronary Artery Disease: JACC Review Topic of the Week. *J Am Coll Cardiol* **73**, 964–976 (2019).
19. Stone, P. H., Libby, P. & Boden, W. E. Fundamental Pathobiology of Coronary Atherosclerosis and Clinical Implications for Chronic Ischemic Heart Disease Management-The Plaque Hypothesis: A Narrative Review. *JAMA Cardiol* (2022) doi:10.1001/jamacardio.2022.3926.
20. Ferraro, R. *et al.* Evaluation and Management of Patients With Stable Angina: Beyond the Ischemia Paradigm: JACC State-of-the-Art Review. *J Am Coll Cardiol* **76**, 2252–2266 (2020).
21. Ali, Z. *et al.* Optical coherence tomography-guided coronary stent implantation compared to angiography: a multicentre randomised trial in PCI - design and rationale of ILUMIEN IV: OPTIMAL PCI. *EuroIntervention* **16**, 1092–1099 (2021).
22. Stone, G. W. *et al.* A prospective natural-history study of coronary atherosclerosis. *N Engl J Med* **364**, 226–35 (2011).

23. Hajhosseiny, R. *et al.* Coronary Magnetic Resonance Angiography: Technical Innovations Leading Us to the Promised Land? *JACC Cardiovasc Imaging* **13**, 2653–2672 (2020).
24. Joshi, N. v *et al.* 18F-fluoride positron emission tomography for identification of ruptured and high-risk coronary atherosclerotic plaques: a prospective clinical trial. *Lancet* **383**, 705–13 (2014).
25. Garcia, S. *et al.* Outcomes after complete versus incomplete revascularization of patients with multivessel coronary artery disease: a meta-analysis of 89,883 patients enrolled in randomized clinical trials and observational studies. *J Am Coll Cardiol* **62**, 1421–31 (2013).
26. Fearon, W. F. *et al.* Fractional Flow Reserve-Guided PCI as Compared with Coronary Bypass Surgery. *N Engl J Med* **386**, 128–137 (2022).
27. Dweck, M. R. *et al.* Imaging of coronary atherosclerosis - evolution towards new treatment strategies. *Nat Rev Cardiol* **13**, 533–48 (2016).
28. Andreini, D. *et al.* Pre-procedural planning of coronary revascularization by cardiac computed tomography: An expert consensus document of the Society of Cardiovascular Computed Tomography. *EuroIntervention* **18**, e872–e887 (2022).
29. Xiong, T.-Y. *et al.* Transcatheter aortic valve implantation in patients with bicuspid valve morphology: a roadmap towards standardization. *Nat Rev Cardiol* **20**, 52–67 (2023).
30. Gorog, D. A. *et al.* Current and novel biomarkers of thrombotic risk in COVID-19: a Consensus Statement from the International COVID-19 Thrombosis Biomarkers Colloquium. *Nat Rev Cardiol* **19**, 475–495 (2022).
31. Alvarenga, A. *et al.* Scenarios for population health inequalities in 2030 in Europe: the EURO-HEALTHY project experience. *Int J Equity Health* **18**, 100 (2019).
32. Veeranki, S. P. *et al.* A Delphi Consensus Approach for Difficult-to-Treat Patients with Severe Hemophilia A without Inhibitors. *J Blood Med* **12**, 913–928 (2021).
33. Dewey, M. *et al.* Clinical quantitative cardiac imaging for the assessment of myocardial ischaemia. *Nat Rev Cardiol* **17**, 427–450 (2020).
34. Budoff, M. J. *et al.* Cardiac CT angiography in current practice: An American society for preventive cardiology clinical practice statement☆. *Am J Prev Cardiol* **9**, 100318 (2022).
35. Wong, N. D. *et al.* Atherosclerotic cardiovascular disease risk assessment: An American Society for Preventive Cardiology clinical practice statement. *Am J Prev Cardiol* **10**, 100335 (2022).
36. Halliburton, S. *et al.* State-of-the-art in CT hardware and scan modes for cardiovascular CT. *J Cardiovasc Comput Tomogr* **6**, 154–63 (2012).
37. Song, Y. bin *et al.* Contemporary Discrepancies of Stenosis Assessment by Computed Tomography and Invasive Coronary Angiography. *Circ Cardiovasc Imaging* **12**, e007720 (2019).
38. Krazinski, A. W. *et al.* Reduced radiation dose and improved image quality at cardiovascular CT angiography by automated attenuation-based tube voltage selection: intra-individual comparison. *Eur Radiol* **24**, 2677–2684 (2014).
39. Dweck, M. R., Puntman, V., Vesey, A. T., Fayad, Z. A. & Nagel, E. MR Imaging of Coronary Arteries and Plaques. *JACC Cardiovasc Imaging* **9**, 306–16 (2016).
40. Schönenberger, E. *et al.* Kidney Injury after Intravenous versus Intra-arterial Contrast Agent in Patients Suspected of Having Coronary Artery Disease: A Randomized Trial. *Radiology* **292**, 664–672 (2019).
41. Bosserdt, M. *et al.* Serum creatinine baseline fluctuation and acute kidney injury after intravenous or intra-arterial contrast agent administration-an intraindividual comparison as part of a randomized controlled trial. *Nephrol Dial Transplant* **37**, 1191–1194 (2022).
42. Bustin, A. *et al.* Five-minute whole-heart coronary MRA with sub-millimeter isotropic resolution, 100% respiratory scan efficiency, and 3D-PROST reconstruction. *Magn Reson Med* **81**, 102–115 (2019).
43. Kato, Y. *et al.* Non-contrast coronary magnetic resonance angiography: current frontiers and future horizons. *MAGMA* **33**, 591–612 (2020).
44. Nagata, M. *et al.* Diagnostic accuracy of 1.5-T unenhanced whole-heart coronary MR angiography performed with 32-channel cardiac coils: initial single-center experience. *Radiology* **259**, 384–92 (2011).
45. Makowski, M. R. *et al.* Characterization of coronary atherosclerosis by magnetic resonance imaging. *Circulation* **128**, 1244–55 (2013).
46. Jansen, C. H. P. *et al.* Detection of intracoronary thrombus by magnetic resonance imaging in patients with acute myocardial infarction. *Circulation* **124**, 416–24 (2011).

47. Ehara, S. *et al.* Hyperintense plaque identified by magnetic resonance imaging relates to intracoronary thrombus as detected by optical coherence tomography in patients with angina pectoris. *Eur Heart J Cardiovasc Imaging* **13**, 394–9 (2012).
48. Tarkin, J. M. *et al.* Imaging Atherosclerosis. *Circ Res* **118**, 750–69 (2016).
49. Hucker, W. J. & Jaffer, F. A. F-FDG PET Imaging of Atherosclerosis-A New Approach to Detect Inflamed, High-Risk Coronary Plaques? *Curr Cardiovasc Imaging Rep* **4**, 1–3 (2011).
50. Sun, Z.-H., Rashmizal, H. & Xu, L. Molecular imaging of plaques in coronary arteries with PET and SPECT. *J Geriatr Cardiol* **11**, 259–73 (2014).
51. Kennedy-Dixon, T.-G., Gossell-Williams, M., Cooper, M., Trabelsi, M. & Vinjamuri, S. Evaluation of Radiopharmaceutical Adverse Reaction Reports to the British Nuclear Medicine Society from 2007 to 2016. *J Nucl Med* **58**, 2010–2012 (2017).
52. Silberstein, E. B. Prevalence of adverse events to radiopharmaceuticals from 2007 to 2011. *J Nucl Med* **55**, 1308–10 (2014).
53. Mayer, M. *et al.* Imaging Atherosclerosis by PET, With Emphasis on the Role of FDG and NaF as Potential Biomarkers for This Disorder. *Front Physiol* **11**, 511391 (2020).
54. Leccisotti, L., Nicoletti, P., Cappiello, C., Indovina, L. & Giordano, A. PET imaging of vulnerable coronary artery plaques. *Clin Transl Imaging* **7**, 267–284 (2019).
55. Verberne, H. J. *et al.* EANM procedural guidelines for radionuclide myocardial perfusion imaging with SPECT and SPECT/CT: 2015 revision. *Eur J Nucl Med Mol Imaging* **42**, 1929–40 (2015).
56. Green, N. E. *et al.* Angiographic views used for percutaneous coronary interventions: a three-dimensional analysis of physician-determined vs. computer-generated views. *Catheter Cardiovasc Interv* **64**, 451–9 (2005).
57. Brugaletta, S. *et al.* NIRS and IVUS for characterization of atherosclerosis in patients undergoing coronary angiography. *JACC Cardiovasc Imaging* **4**, 647–55 (2011).
58. Saito, Y. *et al.* Clinical expert consensus document on standards for measurements and assessment of intravascular ultrasound from the Japanese Association of Cardiovascular Intervention and Therapeutics. *Cardiovasc Interv Ther* **35**, 1–12 (2020).
59. Akasaka, T. *et al.* Pathophysiology of acute coronary syndrome assessed by optical coherence tomography. *J Cardiol* **56**, 8–14 (2010).
60. Araki, M. *et al.* Optical coherence tomography in coronary atherosclerosis assessment and intervention. *Nat Rev Cardiol* **19**, 684–703 (2022).
61. Johnson, T. W. *et al.* Clinical use of intracoronary imaging. Part 2: acute coronary syndromes, ambiguous coronary angiography findings, and guiding interventional decision-making: an expert consensus document of the European Association of Percutaneous Cardiovascular Interventions. *Eur Heart J* **40**, 2566–2584 (2019).
62. Mintz, G. S. & Guagliumi, G. Intravascular imaging in coronary artery disease. *Lancet* **390**, 793–809 (2017).
63. Dewey, M. *et al.* Noninvasive coronary angiography by 320-row computed tomography with lower radiation exposure and maintained diagnostic accuracy: comparison of results with cardiac catheterization in a head-to-head pilot investigation. *Circulation* **120**, 867–75 (2009).
64. von Ballmoos, M. W., Haring, B., Juillerat, P. & Alkadhi, H. Meta-analysis: diagnostic performance of low-radiation-dose coronary computed tomography angiography. *Ann Intern Med* **154**, 413–20 (2011).
65. Kim, W. Y. *et al.* Coronary magnetic resonance angiography for the detection of coronary stenoses. *N Engl J Med* **345**, 1863–9 (2001).
66. Kato, S. *et al.* Assessment of coronary artery disease using magnetic resonance coronary angiography: a national multicenter trial. *J Am Coll Cardiol* **56**, 983–91 (2010).
67. Figtree, G. A. *et al.* Noninvasive Plaque Imaging to Accelerate Coronary Artery Disease Drug Development. *Circulation* **146**, 1712–1727 (2022).
68. Tonino, P. A. L. *et al.* Angiographic versus functional severity of coronary artery stenoses in the FAME study fractional flow reserve versus angiography in multivessel evaluation. *J Am Coll Cardiol* **55**, 2816–21 (2010).
69. Koo, B.-K. *et al.* Fractional Flow Reserve or Intravascular Ultrasonography to Guide PCI. *N Engl J Med* **387**, 779–789 (2022).
70. Mintz, G. S., Matsumura, M., Ali, Z. & Maehara, A. Clinical Utility of Intravascular Imaging: Past, Present, and Future. *JACC Cardiovasc Imaging* **15**, 1799–1820 (2022).
71. Arbab-Zadeh, A. & Hoe, J. Quantification of coronary arterial stenoses by multidetector CT angiography in comparison with conventional angiography methods, caveats, and implications. *JACC Cardiovasc Imaging* **4**, 191–202 (2011).

72. Zir, L. M., Miller, S. W., Dinsmore, R. E., Gilbert, J. P. & Harthorne, J. W. Interobserver variability in coronary angiography. *Circulation* **53**, 627–32 (1976).
73. Nallamothu, B. K. *et al.* Comparison of clinical interpretation with visual assessment and quantitative coronary angiography in patients undergoing percutaneous coronary intervention in contemporary practice: the Assessing Angiography (A2) project. *Circulation* **127**, 1793–800 (2013).
74. Kubo, T. *et al.* OCT compared with IVUS in a coronary lesion assessment: the OPUS-CLASS study. *JACC Cardiovasc Imaging* **6**, 1095–1104 (2013).
75. Nishi, T. *et al.* Head-to-head comparison of quantitative measurements between intravascular imaging systems: An in vitro phantom study. *Int J Cardiol Heart Vasc* **36**, 100867 (2021).
76. Douglas, P. S. *et al.* Outcomes of anatomical versus functional testing for coronary artery disease. *N Engl J Med* **372**, 1291–300 (2015).
77. SCOT-HEART investigators. CT coronary angiography in patients with suspected angina due to coronary heart disease (SCOT-HEART): an open-label, parallel-group, multicentre trial. *Lancet* **385**, 2383–91 (2015).
78. Hajhosseiny, R. *et al.* Clinical comparison of sub-mm high-resolution non-contrast coronary CMR angiography against coronary CT angiography in patients with low-intermediate risk of coronary artery disease: a single center trial. *J Cardiovasc Magn Reson* **23**, 57 (2021).
79. Park, S.-J. *et al.* Intravascular ultrasound-derived minimal lumen area criteria for functionally significant left main coronary artery stenosis. *JACC Cardiovasc Interv* **7**, 868–74 (2014).
80. D'Ascenzo, F. *et al.* Accuracy of intravascular ultrasound and optical coherence tomography in identifying functionally significant coronary stenosis according to vessel diameter: A meta-analysis of 2,581 patients and 2,807 lesions. *Am Heart J* **169**, 663–73 (2015).
81. Mergen, V. *et al.* Ultra-High-Resolution Coronary CT Angiography With Photon-Counting Detector CT: Feasibility and Image Characterization. *Invest Radiol* **57**, 780–788 (2022).
82. Boccalini, S. *et al.* First In-Human Results of Computed Tomography Angiography for Coronary Stent Assessment With a Spectral Photon Counting Computed Tomography. *Invest Radiol* **57**, 212–221 (2022).
83. Küstner, T. *et al.* Deep-learning based super-resolution for 3D isotropic coronary MR angiography in less than a minute. *Magn Reson Med* **86**, 2837–2852 (2021).
84. Yu, W. *et al.* Diagnostic accuracy of intracoronary optical coherence tomography-derived fractional flow reserve for assessment of coronary stenosis severity. *EuroIntervention* **15**, 189–197 (2019).
85. Yu, W. *et al.* Accuracy of Intravascular Ultrasound-Based Fractional Flow Reserve in Identifying Hemodynamic Significance of Coronary Stenosis. *Circ Cardiovasc Interv* **14**, e009840 (2021).
86. Kolossváry, M., Szilveszter, B., Merkely, B. & Maurovich-Horvat, P. Plaque imaging with CT-a comprehensive review on coronary CT angiography based risk assessment. *Cardiovasc Diagn Ther* **7**, 489–506 (2017).
87. Motwani, M. High-risk plaque features on coronary computed tomography angiography: a long-term relationship: it's complicated! *Eur Heart J Cardiovasc Imaging* (2019) doi:10.1093/ehjci/jez253.
88. Rumberger, J. A. & Kaufman, L. A rosetta stone for coronary calcium risk stratification: agatston, volume, and mass scores in 11,490 individuals. *AJR Am J Roentgenol* **181**, 743–8 (2003).
89. Latif, M. A., Budoff, M. J. & Greenland, P. *Cardiac CT*. (Springer Berlin Heidelberg, 2014). doi:10.1007/978-3-642-41883-9.
90. Budoff, M. J. *et al.* Ten-year association of coronary artery calcium with atherosclerotic cardiovascular disease (ASCVD) events: the multi-ethnic study of atherosclerosis (MESA). *Eur Heart J* **39**, 2401–2408 (2018).
91. Hollenberg, E. J. *et al.* Relationship Between Coronary Artery Calcium and Atherosclerosis Progression Among Patients With Suspected Coronary Artery Disease. *JACC Cardiovasc Imaging* **15**, 1063–1074 (2022).
92. Grundy, S. M. *et al.* 2018 AHA/ACC/AACVPR/AAPA/ABC/ACPM/ADA/AGS/APhA/ASPC/NLA/PCNA Guideline on the Management of Blood Cholesterol: Executive Summary: A Report of the American College of Cardiology/American Heart Association Task Force on Clinical Practice Guidelines. *Circulation* **139**, e1046–e1081 (2019).

93. Williams, M. C. *et al.* Low-Attenuation Noncalcified Plaque on Coronary Computed Tomography Angiography Predicts Myocardial Infarction: Results From the Multicenter SCOT-HEART Trial (Scottish Computed Tomography of the HEART). *Circulation* **141**, 1452–1462 (2020).
94. Dweck, M. R. *et al.* Contemporary rationale for non-invasive imaging of adverse coronary plaque features to identify the vulnerable patient: a Position Paper from the European Society of Cardiology Working Group on Atherosclerosis and Vascular Biology and the European Association of Cardiovascular Imaging. *Eur Heart J Cardiovasc Imaging* **21**, 1177–1183 (2020).
95. Greenland, P. & Lloyd-Jones, D. M. Role of Coronary Artery Calcium Testing for Risk Assessment in Primary Prevention of Atherosclerotic Cardiovascular Disease: A Review. *JAMA Cardiol* **7**, 219–224 (2022).
96. Tzolos, E. *et al.* Pericoronary Adipose Tissue Attenuation, Low-Attenuation Plaque Burden, and 5-Year Risk of Myocardial Infarction. *JACC Cardiovasc Imaging* **15**, 1078–1088 (2022).
97. Feger, S. *et al.* Effect of Computed Tomography Versus Invasive Coronary Angiography on Statin Adherence: A Randomized Controlled Trial. *JACC Cardiovasc Imaging* **14**, 1480–1483 (2021).
98. Antonopoulos, A. S. *et al.* Detecting human coronary inflammation by imaging perivascular fat. *Sci Transl Med* **9**, (2017).
99. Sermesant, M., Delingette, H., Cochet, H., Jaïs, P. & Ayache, N. Applications of artificial intelligence in cardiovascular imaging. *Nat Rev Cardiol* **18**, 600–609 (2021).
100. Elnabawi, Y. A. *et al.* Association of Biologic Therapy With Coronary Inflammation in Patients With Psoriasis as Assessed by Perivascular Fat Attenuation Index. *JAMA Cardiol* **4**, 885–891 (2019).
101. Oikonomou, E. K. *et al.* Non-invasive detection of coronary inflammation using computed tomography and prediction of residual cardiovascular risk (the CRISP CT study): a post-hoc analysis of prospective outcome data. *Lancet* **392**, 929–939 (2018).
102. Botnar, R. M. *et al.* Noninvasive coronary vessel wall and plaque imaging with magnetic resonance imaging. *Circulation* **102**, 2582–7 (2000).
103. Kim, W. Y. *et al.* Three-dimensional black-blood cardiac magnetic resonance coronary vessel wall imaging detects positive arterial remodeling in patients with nonsignificant coronary artery disease. *Circulation* **106**, 296–9 (2002).
104. Hays, A. G. *et al.* Local coronary wall eccentricity and endothelial function are closely related in patients with atherosclerotic coronary artery disease. *J Cardiovasc Magn Reson* **19**, 51 (2017).
105. Miao, C. *et al.* Positive remodeling of the coronary arteries detected by magnetic resonance imaging in an asymptomatic population: MESA (Multi-Ethnic Study of Atherosclerosis). *J Am Coll Cardiol* **53**, 1708–15 (2009).
106. Gerretsen, S. *et al.* Detection of coronary plaques using MR coronary vessel wall imaging: validation of findings with intravascular ultrasound. *Eur Radiol* **23**, 115–24 (2013).
107. Noguchi, T. *et al.* High-intensity signals in coronary plaques on noncontrast T1-weighted magnetic resonance imaging as a novel determinant of coronary events. *J Am Coll Cardiol* **63**, 989–99 (2014).
108. Yeon, S. B. *et al.* Delayed-enhancement cardiovascular magnetic resonance coronary artery wall imaging: comparison with multislice computed tomography and quantitative coronary angiography. *J Am Coll Cardiol* **50**, 441–7 (2007).
109. Kawasaki, T. *et al.* Characterization of hyperintense plaque with noncontrast T(1)-weighted cardiac magnetic resonance coronary plaque imaging: comparison with multislice computed tomography and intravascular ultrasound. *JACC Cardiovasc Imaging* **2**, 720–8 (2009).
110. Noguchi, T. *et al.* Effect of Intensive Statin Therapy on Coronary High-Intensity Plaques Detected by Noncontrast T1-Weighted Imaging: The AQUAMARINE Pilot Study. *J Am Coll Cardiol* **66**, 245–256 (2015).
111. Sato, S. *et al.* Coronary High-Intensity Plaques at T1-weighted MRI in Stable Coronary Artery Disease: Comparison with Near-Infrared Spectroscopy Intravascular US. *Radiology* **302**, 557–565 (2022).
112. Dewey, M. Coronary CT versus MR angiography: pro CT--the role of CT angiography. *Radiology* **258**, 329–39 (2011).
113. Mulder, W. J. M. *et al.* Magnetic resonance molecular imaging contrast agents and their application in atherosclerosis. *Top Magn Reson Imaging* **18**, 409–17 (2007).

114. Darçot, E. *et al.* Towards Quantification of Inflammation in Atherosclerotic Plaque in the Clinic - Characterization and Optimization of Fluorine-19 MRI in Mice at 3 T. *Sci Rep* **9**, 17488 (2019).
115. Nazir, M. S. *et al.* High-resolution non-contrast free-breathing coronary cardiovascular magnetic resonance angiography for detection of coronary artery disease: validation against invasive coronary angiography. *J Cardiovasc Magn Reson* **24**, 26 (2022).
116. Tawakol, A. *et al.* Relation between resting amygdalar activity and cardiovascular events: a longitudinal and cohort study. *Lancet* **389**, 834–845 (2017).
117. Cheng, V. Y. *et al.* Coronary arterial 18F-FDG uptake by fusion of PET and coronary CT angiography at sites of percutaneous stenting for acute myocardial infarction and stable coronary artery disease. *J Nucl Med* **53**, 575–83 (2012).
118. Borchert, T. *et al.* Dissecting the target leukocyte subpopulations of clinically relevant inflammation radiopharmaceuticals. *J Nucl Cardiol* **28**, 1636–1645 (2021).
119. Tarkin, J. M. *et al.* Detection of Atherosclerotic Inflammation by 68Ga-DOTATATE PET Compared to [18F]FDG PET Imaging. *J Am Coll Cardiol* **69**, 1774–1791 (2017).
120. Kwiecinski, J. *et al.* Coronary 18F-Sodium Fluoride Uptake Predicts Outcomes in Patients With Coronary Artery Disease. *J Am Coll Cardiol* **75**, 3061–3074 (2020).
121. Ishiwata, Y. *et al.* Quantification of temporal changes in calcium score in active atherosclerotic plaque in major vessels by 18F-sodium fluoride PET/CT. *Eur J Nucl Med Mol Imaging* **44**, 1529–1537 (2017).
122. Fayad, Z. A. *et al.* Safety and efficacy of dalcetrapib on atherosclerotic disease using novel non-invasive multimodality imaging (dal-PLAQUE): a randomised clinical trial. *Lancet* **378**, 1547–59 (2011).
123. Vucic, E. *et al.* Regression of inflammation in atherosclerosis by the LXR agonist R211945: a noninvasive assessment and comparison with atorvastatin. *JACC Cardiovasc Imaging* **5**, 819–28 (2012).
124. van der Valk, F. M. *et al.* Increased haematopoietic activity in patients with atherosclerosis. *Eur Heart J* **38**, 425–432 (2017).
125. US National Library of Medicine. ClinicalTrials.gov. https://clinicaltrials.gov/ct2/show/NCT02278211. Preprint at (2015).
126. Wu, M. *et al.* Feasibility of In Vivo Imaging of Fibroblast Activation Protein in Human Arterial Walls. *J Nucl Med* **63**, 948–951 (2022).
127. Tzolos, E. *et al.* Noninvasive In Vivo Coronary Artery Thrombus Imaging. *JACC Cardiovasc Imaging* (2022) doi:10.1016/j.jcmg.2022.10.002.
128. Derlin, T. *et al.* Exploring Vessel Wall Biology In Vivo By Ultra-Sensitive Total-Body Positron Emission Tomography. *J Nucl Med* (2022) doi:10.2967/jnumed.122.264550.
129. Derlin, T. *et al.* Imaging of chemokine receptor CXCR4 expression in culprit and non-culprit coronary atherosclerotic plaque using motion-corrected [68Ga]pentixafor PET/CT. *Eur J Nucl Med Mol Imaging* **45**, 1934–1944 (2018).
130. Hong, H. *et al.* Radial wall strain: a novel angiographic measure of plaque composition and vulnerability. *EuroIntervention* (2022) doi:10.4244/EIJ-D-22-00537.
131. Neumann, F.-J. *et al.* 2018 ESC/EACTS Guidelines on myocardial revascularization. *Eur Heart J* **40**, 87–165 (2019).
132. Huang, D. *et al.* Assessment of endothelial shear stress in patients with mild or intermediate coronary stenoses using coronary computed tomography angiography: comparison with invasive coronary angiography. *Int J Cardiovasc Imaging* **33**, 1101–1110 (2017).
133. Kröner, E. S. J. *et al.* Positive remodeling on coronary computed tomography as a marker for plaque vulnerability on virtual histology intravascular ultrasound. *Am J Cardiol* **107**, 1725–9 (2011).
134. Waksman, R. *et al.* Identification of patients and plaques vulnerable to future coronary events with near-infrared spectroscopy intravascular ultrasound imaging: a prospective, cohort study. *Lancet* **394**, 1629–1637 (2019).
135. Xu, J. & Lo, S. Fundamentals and role of intravascular ultrasound in percutaneous coronary intervention. *Cardiovasc Diagn Ther* **10**, 1358–1370 (2020).
136. Zhang, J. *et al.* Intravascular Ultrasound Versus Angiography-Guided Drug-Eluting Stent Implantation: The ULTIMATE Trial. *J Am Coll Cardiol* **72**, 3126–3137 (2018).
137. Volleberg, R. *et al.* Optical coherence tomography and coronary revascularization: from indication to procedural optimization. *Trends Cardiovasc Med* (2021) doi:10.1016/j.tcm.2021.10.009.
138. Jodas, D. S., Pereira, A. S. & Tavares, J. M. R. S. Automatic segmentation of the lumen region in intravascular images of the coronary artery. *Med Image Anal* **40**, 60–79 (2017).

139. Souteyrand, G. *et al.* Mechanisms of stent thrombosis analysed by optical coherence tomography: insights from the national PESTO French registry. *Eur Heart J* **37**, 1208–16 (2016).
140. Joner, M. *et al.* Neoatherosclerosis in Patients With Coronary Stent Thrombosis: Findings From Optical Coherence Tomography Imaging (A Report of the PRESTIGE Consortium). *JACC Cardiovasc Interv* **11**, 1340–1350 (2018).
141. Adriaenssens, T. *et al.* Optical Coherence Tomography Findings in Patients With Coronary Stent Thrombosis: A Report of the PRESTIGE Consortium (Prevention of Late Stent Thrombosis by an Interdisciplinary Global European Effort). *Circulation* **136**, 1007–1021 (2017).
142. Shimokado, A. *et al.* In vivo optical coherence tomography imaging and histopathology of healed coronary plaques. *Atherosclerosis* **275**, 35–42 (2018).
143. Akl, E. *et al.* First in-human evaluation of a novel intravascular ultrasound and optical coherence tomography system for intracoronary imaging. *Catheter Cardiovasc Interv* **99**, 686–698 (2022).
144. Araki, M. *et al.* Predictors of Rapid Plaque Progression: An Optical Coherence Tomography Study. *JACC Cardiovasc Imaging* **14**, 1628–1638 (2021).
145. Ali, Z. A. *et al.* Optical coherence tomography compared with intravascular ultrasound and with angiography to guide coronary stent implantation (ILUMIEN III: OPTIMIZE PCI): a randomised controlled trial. *Lancet* **388**, 2618–2628 (2016).
146. Chu, M. *et al.* Artificial intelligence and optical coherence tomography for the automatic characterisation of human atherosclerotic plaques. *EuroIntervention* **17**, 41–50 (2021).
147. Hebsgaard, L. *et al.* Co-registration of optical coherence tomography and X-ray angiography in percutaneous coronary intervention. the Does Optical Coherence Tomography Optimize Revascularization (DOCTOR) fusion study. *Int J Cardiol* **182**, 272–8 (2015).
148. Gardner, C. M. *et al.* Detection of lipid core coronary plaques in autopsy specimens with a novel catheter-based near-infrared spectroscopy system. *JACC Cardiovasc Imaging* **1**, 638–48 (2008).
149. Kakizaki, S. *et al.* Optical Coherence Tomography Fractional Flow Reserve and Cardiovascular Outcomes in Patients With Acute Coronary Syndrome. *JACC Cardiovasc Interv* **15**, 2035–2048 (2022).
150. Gosling, O. *et al.* A comparison of radiation doses between state-of-the-art multislice CT coronary angiography with iterative reconstruction, multislice CT coronary angiography with standard filtered back-projection and invasive diagnostic coronary angiography. *Heart* **96**, 922–6 (2010).
151. Herzog, B. A. *et al.* First head-to-head comparison of effective radiation dose from low-dose 64-slice CT with prospective ECG-triggering versus invasive coronary angiography. *Heart* **95**, 1656–61 (2009).
152. Dorbala, S. *et al.* SNMMI/ASNC/SCCT guideline for cardiac SPECT/CT and PET/CT 1.0. *J Nucl Med* **54**, 1485–507 (2013).
153. Beheshti, M. *et al.* (18)F-NaF PET/CT: EANM procedure guidelines for bone imaging. *Eur J Nucl Med Mol Imaging* **42**, 1767–1777 (2015).
154. Dewey, M., Schink, T. & Dewey, C. F. Frequency of referral of patients with safety-related contraindications to magnetic resonance imaging. *Eur J Radiol* **63**, 124–7 (2007).
155. Dewey, M., Schink, T. & Dewey, C. F. Claustrophobia during magnetic resonance imaging: cohort study in over 55,000 patients. *J Magn Reson Imaging* **26**, 1322–7 (2007).
156. Napp, A. E. *et al.* Analysis and Prediction of Claustrophobia during MR Imaging with the Claustrophobia Questionnaire: An Observational Prospective 18-month Single-Center Study of 6500 Patients. *Radiology* **283**, 148–157 (2017).
157. Hausmann, D. *et al.* The safety of intracoronary ultrasound. A multicenter survey of 2207 examinations. *Circulation* **91**, 623–30 (1995).
158. van der Sijde, J. N. *et al.* Safety of optical coherence tomography in daily practice: a comparison with intravascular ultrasound. *Eur Heart J Cardiovasc Imaging* **18**, 467–474 (2017).
159. Stuber, M., Börnert, P., Spuentrup, E., Botnar, R. M. & Manning, W. J. Selective three-dimensional visualization of the coronary arterial lumen using arterial spin tagging. *Magn Reson Med* **47**, 322–329 (2002).
160. Stuber, M., Botnar, R. M., Spuentrup, E., Kissinger, K. v. & Manning, W. J. Three-dimensional high-resolution fast spin-echo coronary magnetic resonance angiography. *Magn Reson Med* **45**, 206–211 (2001).

Key references (sorted in the order of appearance)

1. DISCHARGE Trial Group et al. CT or Invasive Coronary Angiography in Stable Chest Pain. N Engl J Med 386, 1591–1602 (2022). Among patients referred for ICA because of stable chest pain and intermediate pre-test probability of CAD, the risk of major procedure-related complications during patient management was lower in the CT than in the ICA group.

2. Perera D. et al. Percutaneous Revascularization for Ischemic Left Ventricular Dysfunction. N Engl J Med 387:1351-1360 (2022). The REVIVED study demonstrated that in patients with severe ischaemic left ventricular disfunction, revascularisation with PCI did not show a lower incidence of death or hospitalisation for heart failure in comparison to optimal medical therapy.

3. Maron DJ. et al. Initial Invasive or Conservative Strategy for Stable Coronary Disease. N Engl J Med (2020). The ISCHEMIA trial that showed that in stable CAD patients with moderate or severe myocardial ischaemia, an initial invasive treatment strategy did not show a reduction in risk of cardiovascular events or any causes of death over a median of 3.2 years.

4. Stone, P. H. et al. Fundamental Pathobiology of Coronary Atherosclerosis and Clinical Implications for Chronic Ischemic Heart Disease Management-The Plaque Hypothesis: A Narrative Review. *JAMA Cardiol* (2022) doi:10.1001/jamacardio.2022.3926. This review by Stone P.H. et al. discuss the current hypothesis of coronary atherosclerosis taking into account the underlying pathobiologic mechanisms, diagnostic and therapeutical implications, and the approaches for management optimization in patients with chronic coronary disease.

5. Stone, G. W. et al. A prospective natural-history study of coronary atherosclerosis. N Engl J Med 364, 226–35 (2011). In the PROSPECT study of patients who presented with acute coronary syndrome and underwent PCI, major adverse cardiovascular events during follow-up were equally attributable to recurrence at sites of culprit lesions and to nonculprit lesions at other sites.

6. Fearon, W. F. et al. Fractional Flow Reserve-Guided PCI as Compared with Coronary Bypass Surgery. N Engl J Med 386, 128–137 (2022). The FAME-3 trial investigated patients with three-vessel coronary disease, showing that FFR-guided PCI was not inferior to CABG for MACE at 1 year.

7. Williams, M. C. et al. Low-Attenuation Noncalcified Plaque on Coronary Computed Tomography Angiography Predicts Myocardial Infarction: Results From the Multicenter SCOT-HEART Trial (Scottish Computed Tomography of the HEART). Circulation 141, 1452–1462 (2020). In patients presenting with stable chest pain, low-attenuation plaque burden measured by CT is the strongest predictor of subsequent fatal or nonfatal myocardial infarction.

8. Sato, S. *et al*. Coronary High-Intensity Plaques at T1-weighted MRI in Stable Coronary Artery Disease: Comparison with Near-Infrared Spectroscopy Intravascular US. *Radiology* **302**, 557–565 (2022). Sato, S

et al. demonstrated that high-intensity plaques in T1-weighted MRI were predominantly caused by intra-plaque haemorrhage; these findings were correlated with NIRS/ IVUS of the target vessel.

9. Prediction of Recurrent Events With 18F-Fluoride (PREFFIR). ClinicalTrials.gov. https://clinicaltrials.gov/ct2/show/NCT02278211. (2015). The objective of this study was to determine the prediction of recurrent events with 18F-fluoride to identify ruptured and high-risk coronary artery plaques in patients with myocardial infarction.

10. Waksman, R. et al. Identification of patients and plaques vulnerable to future coronary events with near-infrared spectroscopy intravascular ultrasound imaging: a prospective, cohort study. Lancet 394, 1629–1637 (2019). This study demonstrated that NIRS could detect plaque with high risk of rupture (and resulting MACE) based on their elevated lipid content.

11. Zhang, J. et al. Intravascular Ultrasound Versus Angiography-Guided Drug-Eluting Stent Implantation: The ULTIMATE Trial. J Am Coll Cardiol 72, 3126–3137 (2018). In all-comers, it was demonstrated that the use of IVUS guidance during the implantation of drug-eluting stents was associated with a lower rate of cardiovascular deaths compared with ICA guidance.

12. Ali, Z. A. et al. Optical coherence tomography compared with intravascular ultrasound and with angiography to guide coronary stent implantation (ILUMIEN III: OPTIMIZE PCI): a randomised controlled trial. Lancet 388, 2618–2628 (2016). The ILUMIEN III: trial demonstrated comparable optimisation of stent placement for IVUS and OCT, showing similar minimum stent area in both study arms.

Tables

Table 1 | **Technical comparison of imaging tools for direct visualisation of coronary stenosis and atherosclerosis.**

Parameter	CT	MRI	PET	SPECT	ICA	IVUS	OCT
General							
Ionising radiation	Yes, the median effective dose of CT is approximately 2-5 mSv[63,150,151].	No	Yes, effective dose of approximately 10 mSv for the combination of coronary CT angiography, attenuation-correction CT and the radiotracer (0.019 mSv/MBq for 18F-FDG and 0.024 mSv/MBq for 18F-sodium fluoride (NaF))[152,153].	Yes, but no clinical coronary imaging application at present.	Yes, the median effective dose of ICA was reported to be 4.1 mSv[4].	Not by itself, ionising radiation used during the ICA procedure	Not by itself, ionising radiation used during the ICA procedure
Contrast agent, tracer, or non-contrast technique	High iodine concentration (~ 350–400 mg iodine/ml), intravenous administration with a rate of acute kidney injury of 5.6%	Coronary MRI angiography: non-contrast-enhanced 3D bSSFP/T1-GRE sequence Coronary MRI plaque: motion-corrected RD T1-GRE thrombus: MRDTI	Plaque imaging: Calcification: ^{18}F-sodium fluoride (NaF). Glucose metabolism: ^{18}F-FDG. SSTR2: ^{68}Ga-DOTATATE	Currently NA for atherosclerosis assessment. Stenosis can be assessed by the CT component of the procedure.	Iodine contrast agent, intraarterial administration with a significantly higher rate of acute kidney injury of 13.2% compared to CT[40].	NA	Need of clearing during pullbacks (contrast or eventually saline in CKD)
Risk assessment	Only 0.05% (1/1782) of coronary CT in the DISCHARGE trial were associated with a major procedural complication[4]. Major procedural complications of CT and related procedures during the initial subsequent management occurred at a rate of 0.5% in patients with stable chest pain in the DISCHARGE trial - significantly less frequent compared to the 1.9% for the ICA group[4].	Referral of patients with absolute contraindications (e.g. shrapnels and pacemakers) can be a safety concern and occurs at a rate of 0.4%[154]. Claustrophobia is common during MRI with rates between 2% in the outpatient setting[155] and 10% in the inpatient setting[156].	Similar risks as noted for coronary CT plus the risks of the PET tracer. The incidence of radiopharmaceutical adverse events has been reported to be as low as 2.1 to 3.1 per 100,000 administrations (including cutaneous (rash, flush) and cardiovascular (e.g., hypotension, anaphylactoid) reactions), with no deaths[51,52].	No clinical coronary imaging application at present.	1.0% (15/1532) of ICA without PCI and 5.6% of ICA with PCI (15/269) in the DISCHARGE trial were associated with a major procedural complication[4]. Major procedural complications of ICA and related procedures during the initial subsequent management occurred at a rate of 1.9% in the DISCHARGE trial which was significantly more frequent compared to the 0.5% for the CT group[4].	IVUS entails the risks of ICA plus additional IVUS procedure-related risks. Coronary vasospasm is the most common major procedural complication of IVUS (approximately 3%) and pretreatment with nitrates is recommended. Additional major procedure-related complications (dissection, vessel occlusion, embolism) are rare (0.4%)[157].	OCT entails the risks of ICA plus additional OCT procedure-related risks. The rate of major procedural complications related to OCT is similar to that of IVUS[158].
Temporal resolution (acquisition time per frame)	Approximately 150-200 ms	20-60 ms	5s -10s	5 s to 5 min	1-10 ms	30-100 frames per second	180-200 frames per second
Spatial resolution (image analysis voxel size)	0.35*0.35 mm^2(axial) with slice thickness of 0.5 to 0.7 mm	Coronary MRI angiography: 0.9-1.3 mm^3 Coronary MRI plaque imaging: 0.8-1.5 mm^3	Axial resolution: 3-5 mm	Axial resolution: 6-10 mm	0.1-0-2 mm	Axial resolution: 100 to 150 µm; lateral resolution 150 to 300 µm	Axial resolution: 10–15 µm; lateral resolution: 20 to 90 µm
Penetration depth	NA	NA	NA	NA	NA	4-8 mm	0.4-2.0 mm (depending on type of tissue at selected location)
Technical challenges							
Susceptibility to artefacts	Medium	Medium	High	High	Low	Medium	Medium
Small-vessel assessment	Medium	Low	Low	Low	High	Medium	Medium

User dependency	Low	High	Low	Low	Medium	High	High
Need for ECG-gating	Yes	Yes	Yes	Yes	No	No	No
Need of sedation	No	No	No	No	Yes, conscious sedations possible	Yes, conscious sedation possible	Yes, conscious sedation possible
Advantages and disadvantages							
Advantages	Non-(minimally) invasive. Coronary lumen and coronary wall assessment. Similar amount of contrast agent as in ICA.	Inflammation detection in coronary plaque. No need for ionising radiation. Most techniques do not require contrast agent.	Molecular characterisation of pathobiology. Direct inflammation detection in coronary plaque. Calcification activity assessment.	NA	High accuracy in stenosis assessment. Able to assess small vessels. Treatment option during the same procedure.	Higher penetration compared to OCT, enables assessment of all vessel layers.	Higher spatial and temporal resolution than IVUS enables better endoluminal evaluation of plaque. Can penetrate calcium and measure its components.
Disadvantages	High and irregular heart rates. High coronary calcium load and blooming artefacts (false positives).	Challenges due to motion and spatial resolution. Clinical role still to be defined.	Challenges due to motion and limited resolution. Limited availability (in specialised centres only).	Currently no role for SPECT in coronary plaque and stenosis imaging	Invasive user-dependent procedure. No direct assessment of coronary plaque.	Lower temporal and spatial resolution than OCT that limits assessment of superficial plaque components. Challenging to handle in very tortuous vessels and in presence of high-grade stenosis.	Lower penetration that limits assessment of deep vessel layers. Requires clearing of blood during pull-back. Challenging to handle in very tortuous and distal vessels. Cannot penetrate highly scattering, highly attenuating lipid tissue.

Consensus on the technical assessment of imaging modalities compiled in this table was accomplished using the Delphi method with ratings by 10 investigators (1 cardiologist, 5 radiologists, 1 dual certified cardiologist–radiologist, 1 nuclear medicine physician and 2 methodologists).

3D: three-dimensional; bSSFP: balanced steady-state free precession; CT: computed tomography; CKD: chronic kidney disease; ECG: electrocardiogram; F:fluoride; FDG: fluorodeoxyglucose; Ga: gallium; GRE: gradient echo sequence; ICA: invasive coronary angiography; IVUS: intravascular ultrasound; MRI: magnetic resonance imaging; MRDTI: magnetic resonance direct thrombus imaging; OCT: optical coherence tomography; PET: positron emission tomography; RD : respiratory dynamic; SPECT: single-photon emission computed tomography NA, not applicable; SSTR2: somatostatin receptor 2

Figures

Fig. 1 | **Main differences in the revascularisation concepts between PCI and CABG.**

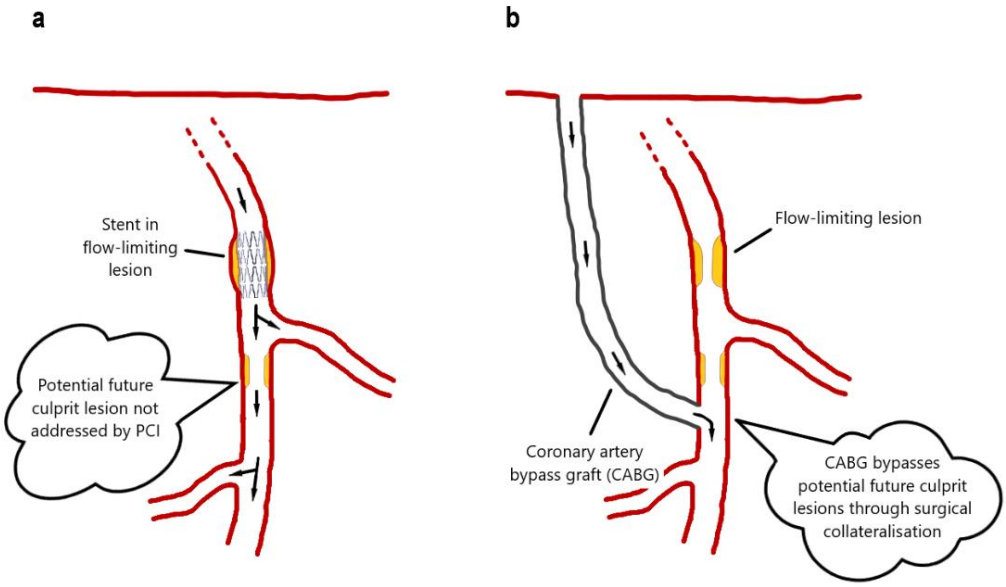

a | Percutaneous coronary intervention (PCI) has the advantage of re-establishing coronary artery blood flow after angioplasty and stent placement in a flow-limiting lesion; however, non-obstructive coronary potential future culprit lesions downstream are not treated, which could lead to infarction in distal vascular territories. **b** | On the other hand, coronary artery bypass grafting (CABG) is a surgical procedure providing a bypass for alternative blood supply to distal coronary territories (usually from a mammary or radial artery), which has the advantage of protecting distal vascular territories as the grafts are usually inserted distal to additional plaque (adapted from Doenst et al.[18]).

Fig. 2 | **Targets of clinical coronary stenosis and atherosclerosis imaging.**

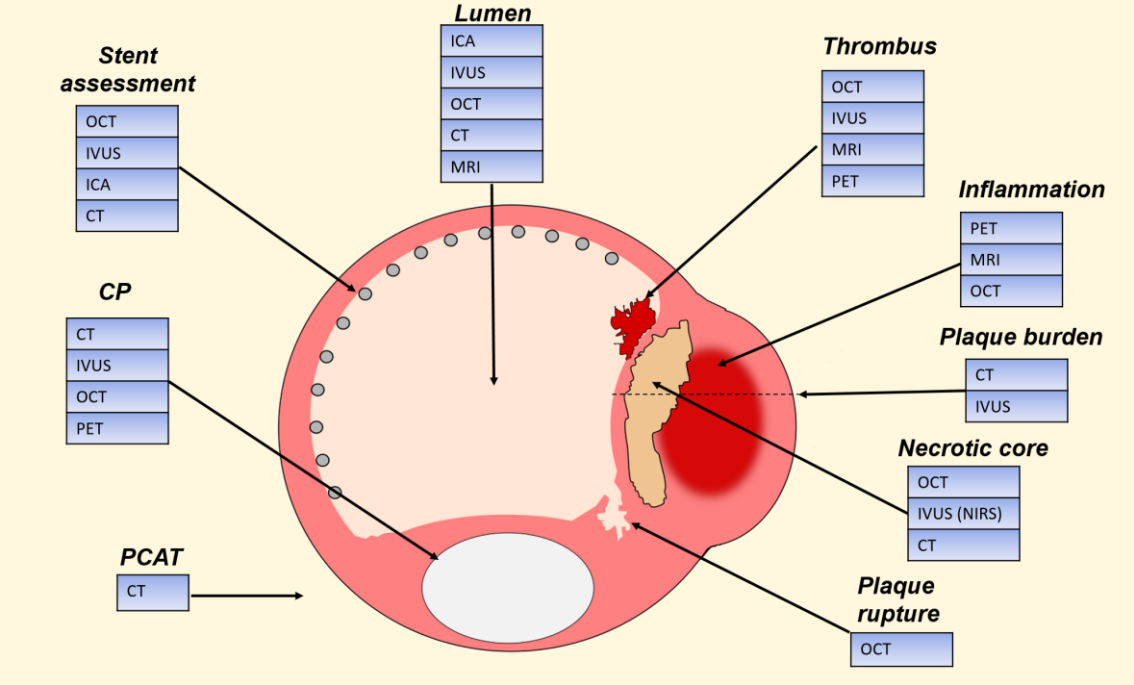

The figure shows a schematic coronary artery cross-section and summarises the different coronary stenosis and atherosclerosis imaging targets (indicated in *Italic* and ***Bold***) and the appropriateness of each imaging modality for each target based on the QCI consensus. The appropriateness is shown in descending order for each of the imaging targets. CT is an appropriate modality to assess plaque burden, coronary plaque (CP), coronary artery lumen dimensions (i.e., stenosis), and pericoronary adipose tissue (PCAT) and may allow assessment of the necrotic core as low-attenuation plaque as well as coronary stents. MRI can be used to assess inflammation and thrombi in a research setting. PET is the best technology to show and quantify coronary artery plaque inflammation and can also identify coronary thrombi though at lower accuracy compared with OCT and IVUS. ICA is the reference standard to assess coronary lumen dimensions and basic stent characteristics. IVUS is appropriate to assess lumen dimensions, plaque composition, thrombi, CP, and stents. OCT is a high-resolution technique to assess coronary plaque rupture, the necrotic core, thrombi, and stents.

CP: calcified plaque; CT: computed tomography; ICA: invasive coronary angiography; IVUS: intravascular ultrasound; MRI: magnetic resonance imaging; NCP: non-calcified plaque; NIRS: near-infrared spectroscopy; OCT: optical-coherence tomography; PET: positron-emission tomography.

Fig. 3 | **Clinical characteristics and appropriateness of coronary artery stenosis and atherosclerosis imaging.**

General clinical characteristics of coronary artery **stenosis and atherosclerosis** imaging modalities	**CT**	**MRI**	**PET**	**SPECT**	**ICA**	**IVUS**	**OCT**
Availability of modality in clinical practice	9	6	4	5	9	6	5
Modality is commonly applied in clinical practice	8	5	2	4	9	5	4
Modality includes quantification in clinical practice	8	5	5	4	7	7	7
Cost-effectiveness of imaging technique	8	5	3	4	6	5	5
General adverse events profile	8	8	7	7	6	5	5

Specific indications: appropriateness of coronary artery **stenosis and atherosclerosis** imaging	**CT**	**MRI**	**PET**	**SPECT**	**ICA**	**IVUS**	**OCT**
Stable chest pain with suspected CAD and intermediate pre-test probability (10-60%)	9	6	4	5	5	3	3
Stable chest pain with suspected CAD and high pre-test probability (>60%)	7	6	4	4	8	6	6
Following an inconclusive or nondiagnostic functional test	8	5	4	4	7	5	5
Acute coronary syndrome without ST elevation	7	4	3	3	8	6	6
Acute coronary syndrome with ST elevation	3	2	1	1	9	7	7
Asymptomatic subjects with high-risk of cardiovascular disease (>10% risk of cardiovascular events in the subsequent 10 years)	7	4	2	2	2	2	2
New symptoms in patients with prior coronary stenting	7	5	4	5	8	6	6
New symptoms following coronary artery bypass grafting	8	6	4	4	7	5	5

Specific groups of patients: appropriateness of coronary artery **stenosis and atherosclerosis** imaging	**CT**	**MRI**	**PET**	**SPECT**	**ICA**	**IVUS**	**OCT**
Female patients	8	7	5	5	7	7	7
Young age (<55y)	8	7	4	4	6	5	5
High heart rate (>70 beats per min)	7	6	5	5	8	7	7
High BMI (>30 kg/m²)	7	6	5	5	7	7	7
Valvular heart disease (including planned transcatheter aortic valve implantation)	9	6	3	2	7	5	4
After heart transplantation	8	6	4	4	7	6	6
Chronic kidney disease (GFR: <30 ml/min/1.73 m²)	6	6	5	5	6	5	5

Specific questions for the evaluation of pathophysiology for clinical quantitative imaging tools							
Coronary artery **stenosis** imaging: specific pathophysiology questions	**CT**	**MRI**	**PET**	**SPECT**	**ICA**	**IVUS**	**OCT**
Coronary artery anatomy (including anomalies)	9	6	3	2	7	3	3
Accuracy of coronary artery stenosis measurement	8	5	2	1	8	8	9
Susceptibility of stenosis measurement to artifacts	6	5	4	4	7	7	6

Coronary **atherosclerosis** imaging: specific pathophysiology questions	**CT**	**MRI**	**PET**	**SPECT**	**ICA**	**IVUS**	**OCT**
Coronary plaque morphology	8	5	2	1	5	8	9
Coronary plaque composition	8	5	2	1	3	8	8
Total coronary plaque burden	9	5	3	2	6	7	6
Culprit coronary plaque detection	7	5	4	2	7	8	8
Coronary plaque inflammation	6	5	7	2	2	5	6
Pericoronary adipose tissue	8	5	4	3	1	3	3

The values shown are the median ratings of the 31 experts at the end of the 3-round clinical Delphi process for each modality and each of the 29 clinical questions. Consensus was rated on a scale of 1 to 9, with 1 to 3 being inappropriate (purple), 4 to 6 being uncertain (yellow), and 7 to 9 being appropriate (green). A total of 31 experts participated. Two radiologists (M.D. and A.J.V.M.), one MD/PhD (F.B.), one cardiologist (D.E.N.), and one biomedical engineer (B.F.) defined the 29 questions in the table. M.D. D.E.N., B.F., and the additional 28 experts answered the questionnaire.

Fig. 4 | **Imaging modalities for the assessment of coronary stenosis.**

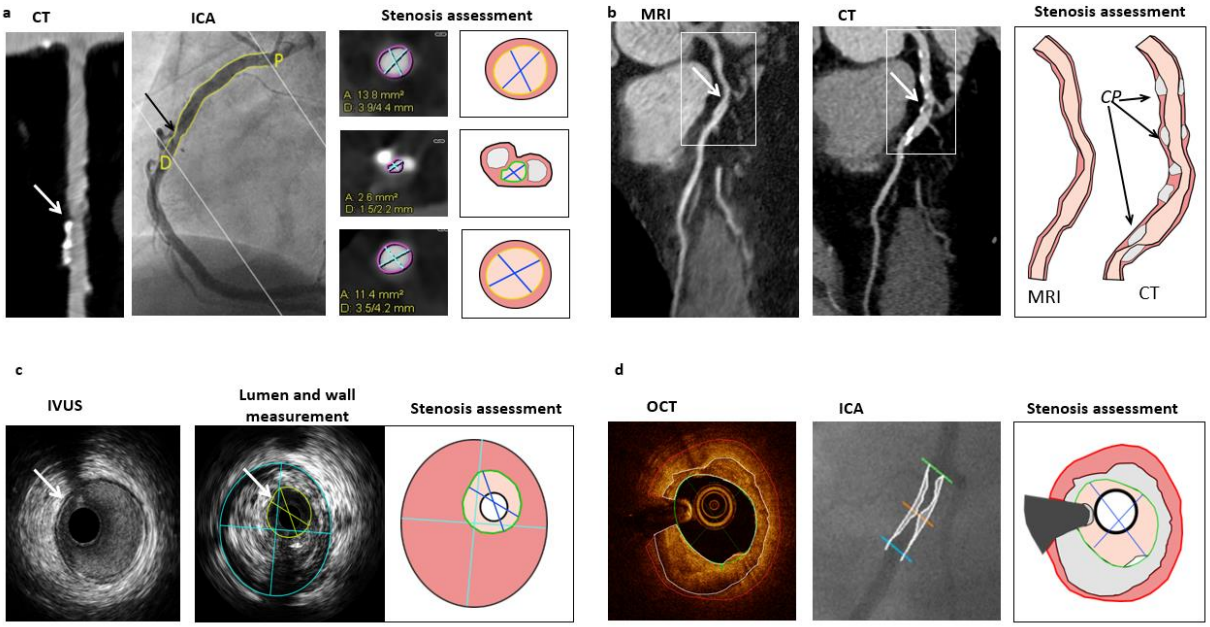

a | Coronary CT image obtained in a 62-year-old male patient with atypical chest pain and severe aortic stenosis. Straight reformation (left panel) of the right coronary artery (RCA) demonstrates several calcified plaques and a 40% diameter stenosis of the mid RCA (arrow), which is confirmed by invasive coronary angiography (ICA)(arrow) (middle panel). The stenosis severity (right panel) is based on the ratio of either the minimal lumen diameter (MLD) or minimal lumen area (MLA) of the stenotic region (red line) and the average luminal diameter of the reference regions (blue lines), respectively. In this case, the MLA was 1.5 mm^2 divided by the average of the area of the reference regions (3.7 mm^2) and multiplied by 100 yields a 40% stenosis. **b**| Coronary MRI demonstrates a curved reformation (left panel) of the left anterior descending coronary artery (LAD). Note that - in comparison to the coronary CT image from the same patient (middle panel) - the lumen of the mid LAD is visually less stenotic because of the lack of signal of calcified plaques. In CT, the lumen of the mid LAD appears difficult to accurately assess due to blooming artefacts caused by calcified plaques. Both imaging modalities identified a >50 stenosis in the proximal LAD (white arrow). The right panel demonstrates a difference in lumen dimensions between both MRI and CT. **c** | IVUS cross-sectional image from the right coronary artery in a case without coronary artery disease. Notice that, in normal coronary vessels, the wall is shown as a thin echogenic layer (arrow) delimited by two low-echogenic layers that correspond to the intima and adventitia (left panel). In comparison, an obstructive coronary plaque in the RCA (middle panel) with a thickened wall causes a 50% diameter stenosis. Assessment of stenosis severity by IVUS (right panel) can be estimated as MLA (green line) or MLD (blue lines); note that the high penetration depth of IVUS allows the visualisation of the outer layers of the vessel wall. **d** | Cross-sectional OCT image from the mid segment of the LCx for assessment of an obstructive lesion with a stenosis area of 81% and stenosis diameter of 56.4% (left panel). Quantitative coronary angiography (middle panel) yields a stenosis area of 95.8% and stenosis diameter of 79.5% illustrating that lumen dimensions measured by OCT are larger, yielding a less severe stenosis grade compared with ICA [74]. The graphical representation of the OCT axial image (right panel) compares estimation of the stenotic lesion based on MLA (green line) and MLD (blue lines) determined in the stenotic segment.

Fig. 5 | **CT for quantitative coronary atherosclerosis imaging.**

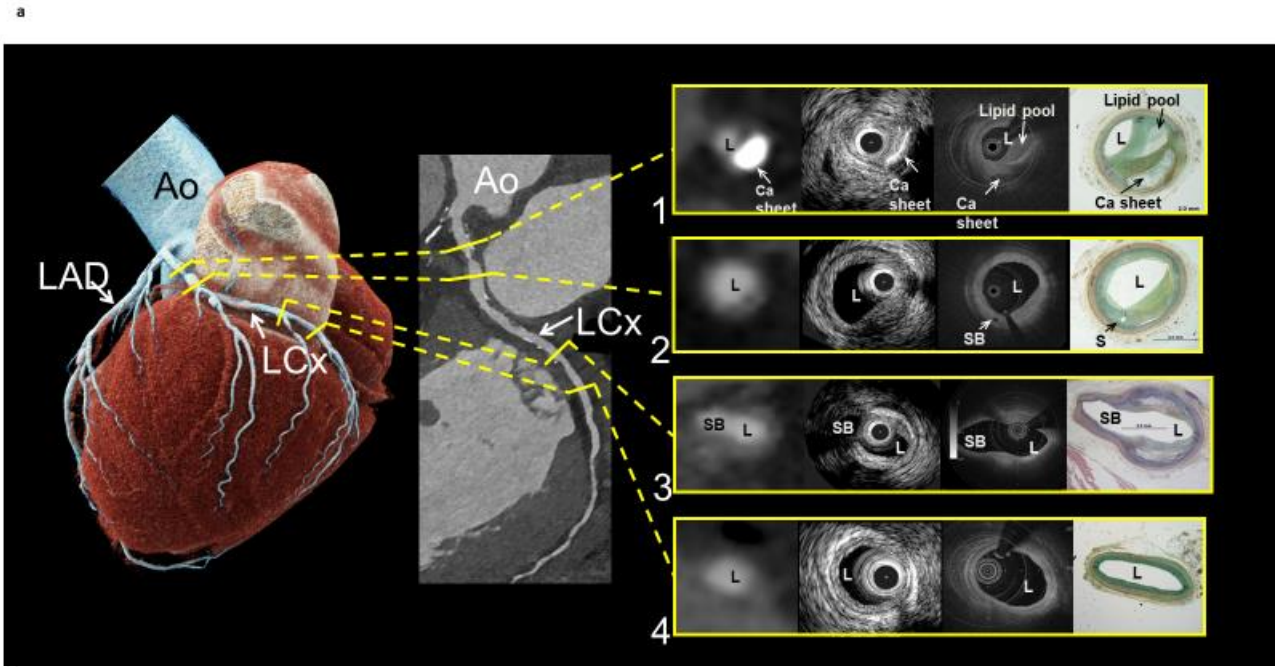

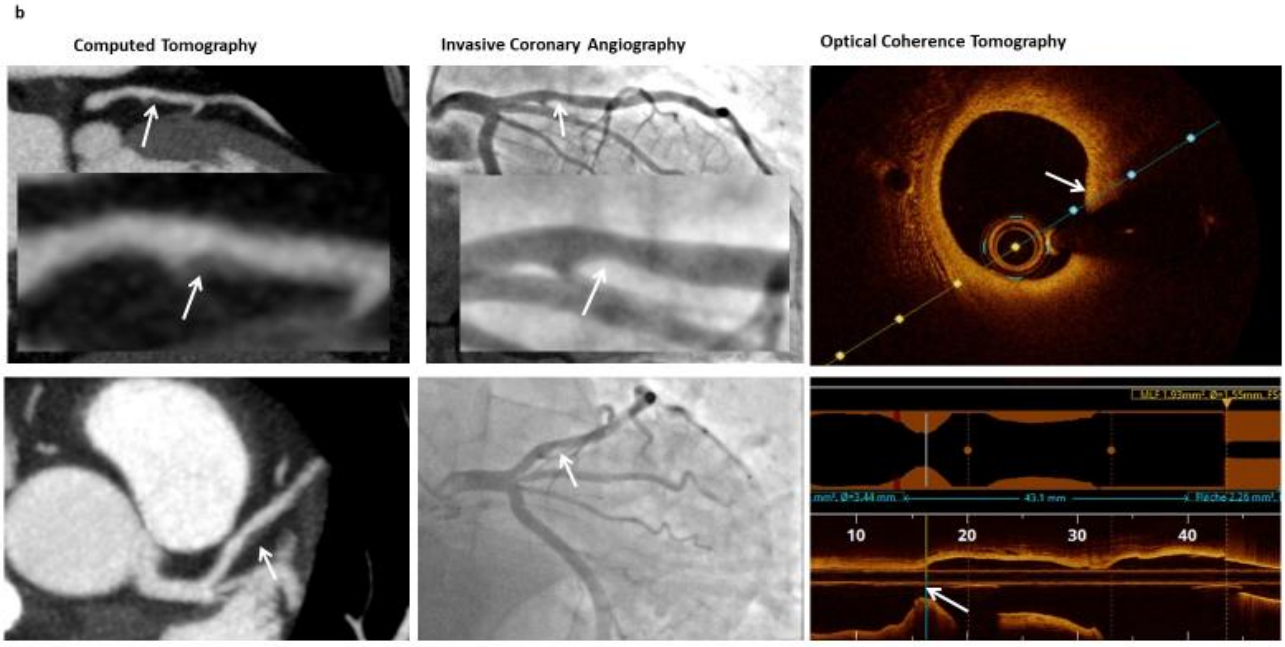

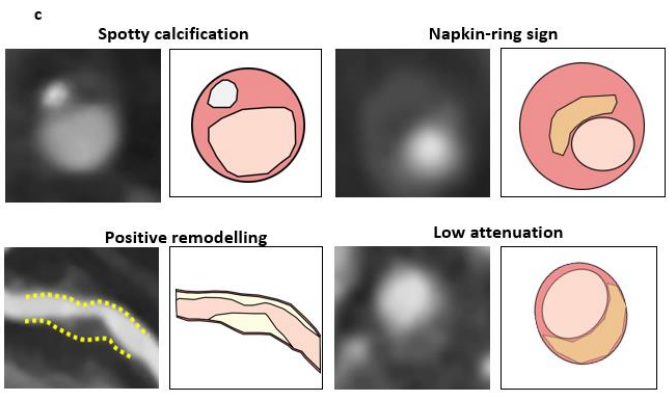

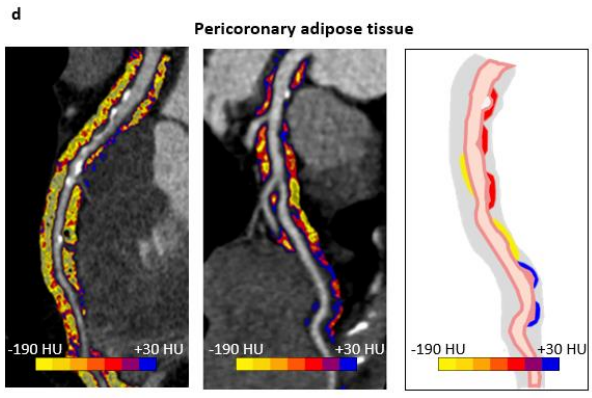

a | Example of plaque characterisation using coronary computed tomography (CT) angiography, intravascular ultrasound (IVUS), optical coherence tomography (OCT), and histology. The left panel shows a volume-rendered CT data set and the middle panel a coronary CT curved multiplanar reconstruction of the left circumflex coronary artery (LCx). The coronary CT of a 62-year-old man with atypical chest pain was acquired in a photon-counting detector CT scanner and reconstructed using 0.2 mm slice thickness. The right panel shows the coronary artery cross-sections from the sites indicated with yellow interrupted lines in the left and middle panels. The images shown in the right panel were acquired as part on an ex vivo investigation (courtesy of Cardiovascular Imaging Research Center, Massachusetts General Hospital, Harvard Medical School, Boston, MA). In the right panel, the images included in the rows represent CT (left), IVUS (middle left), OCT (middle right), and histology (right). Cross-sections are numbered in rows (1-4): fibroatheroma with sheet calcification and lipid pool (row 1). Fibrous plaque and a small side branch (row 2). Early fibroatheroma and a large side branch (row 3). Adaptive intimal thickening (row 4).

b | Correlation of CT findings with ICA and OCT in a 44-year-old male patient presenting with atypical angina. CT shows a low-attenuation plaque in the left anterior descending coronary artery (LAD) (arrows and inset) without significant obstructions. Invasive coronary angiography (ICA) confirms the absence of coronary obstructions and shows luminal narrowing at the location of the high-risk plaque on CT (arrows and inset). OCT was performed as an add-on to ICA and definitely ruled out plaque rupture. The patient was discharged with the recommendation to intensify risk factor modification and with a prescription of high-dose statins based on the findings of a high-risk coronary plaque with low attenuation on CT. **c |** High-risk plaque features. Coronary CT is able to detect features related to risk of rupture and future major adverse cardiovascular events. Spotty calcification is a marker of ongoing inflammation, while the napkin-ring sign, positive remodelling, and low attenuation indicate necrotic cores, which have a higher risk of rupture (**FIG. 2**). **d |** Pericoronary adipose tissue (PCAT) surrounding the coronary arteries on CT has emerged as a new approach to detecting and quantifying coronary artery inflammation to quantify coronary artery inflammation and cardiovascular risk. PCAT is calculated from the attenuation maps around right coronary (RCA), superimposed on the CT images, and presented as a visual colour scale in the left and middle panels (yellow=low, red=high, blue=very high). A higher value is related to inflammation, which can be related to active plaque inflammation with a higher risk of rupture.

Ca: calcium; L: lumen; SB: side branch.

Fig. 6 | **MRI for quantitative coronary atherosclerosis imaging.**

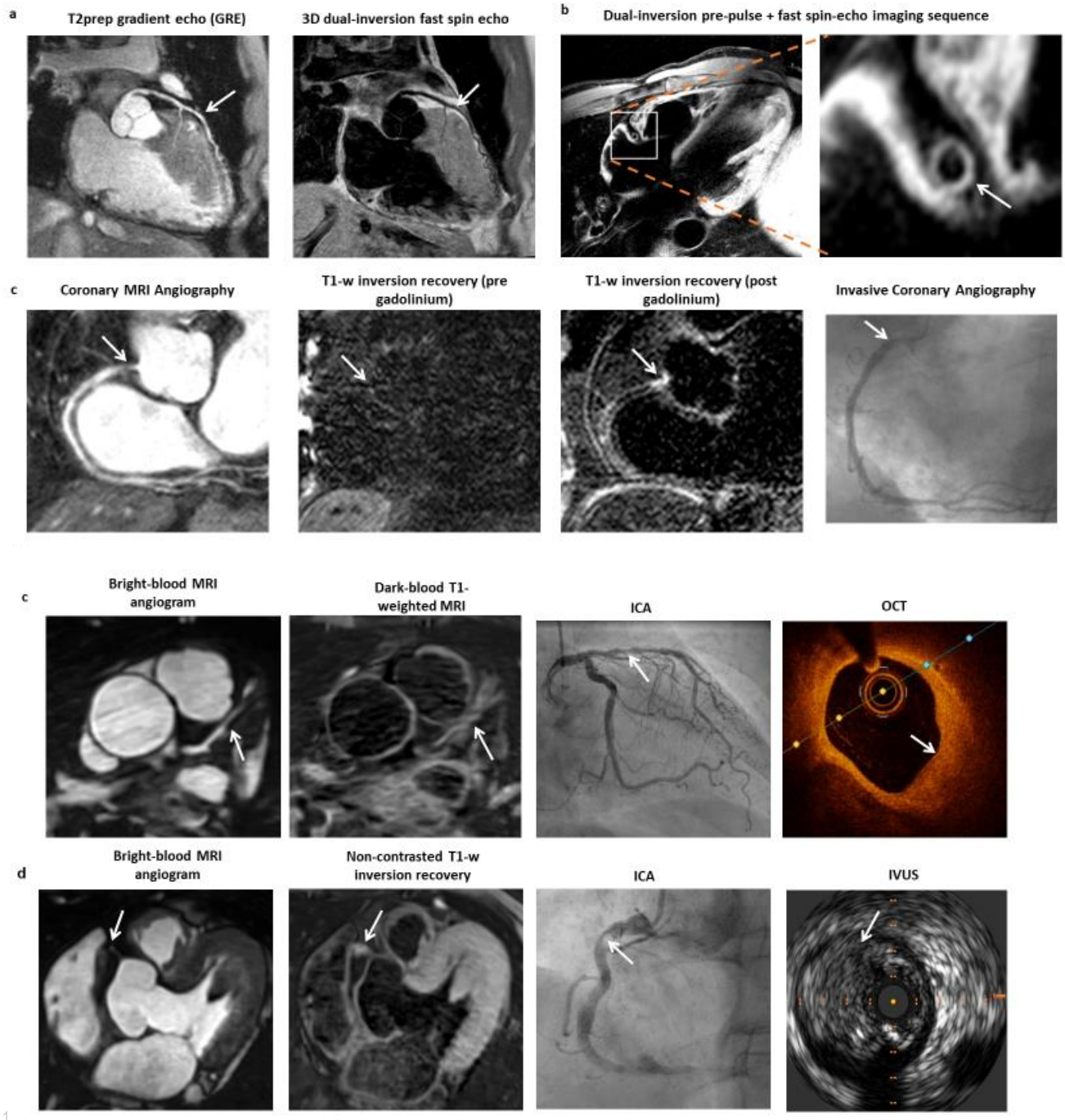

a| Contrast enhancement mechanisms in free-breathing 3D coronary MRI angiography. T2prep gradient echo image (left panel) showing the left anterior descending artery (LAD) with high-intensity signal lumen (arrow) (Adapted from Stuber M, et al.[159]). The same LAD is also visualised with a 3D dual-inversion fast spin echo sequence (right panel), in which the lumen has low signal intensity (middle-right and right panels, arrow) (Adapted from Stuber M et al. [160]). **b** | Coronary vessel walls can be assessed using a dual-inversion pre-pulse in conjunction with a fast spin-echo imaging sequence (left panel). Magnification (right panel) of the right coronary artery (RCA) on an axial plane allows visualisation of the coronary artery wall (arrow). **c** | Coronary MRI angiography (left panel) shows a stenotic atherosclerotic lesion in the proximal RCA (arrow). The pre-contrast inversion-recovery (IR) image of the RCA (middle-left panel) shows no visible coronary enhancement. However, the gadolinium (Gd)-enhanced inversion-recovery image (middle-right

panel) from the same anatomical location shows distinct signal enhancement in the area of the stenotic lesion (arrow). Invasive coronary angiography (ICA) confirms the lesion in the proximal RCA (right, panel, arrow). **d** | Bright-blood MRI angiography (left panel) shows a stenotic lesion in the LAD (arrow), during the simultaneous, interleaved and co-registered dark-blood T1-weighted MRI sequence (middle left panel) the same lesion shows a high-intensity signal (arrow) that can be attributed to a bystander atheromatous plaque. The severity of the lesion is corroborated with the ICA (middle right panel) of the same lesion (arrow) and shown as diffuse plaque with fibroatheroma (arrow) in the OCT cross-sectional image (right panel). **e** | The bright-blood MRI angiogram (left panel) shows a low-intensity signal stenotic lesion in the proximal RCA (arrow), which shows a high-intensity signal (arrow) in the simultaneous, interleaved and co-registered non-contrast T1-weighted inversion recovery sequence (middle left panel) related to acute plaque rupture/thrombus (**FIG. 2**). The stenosis severity of the lesion (arrow) is corroborated by ICA (middle right panel) and shown as an acute intraluminal thrombus (arrow) in the IVUS cross-sectional image (right panel).

Fig. 7 | **PET for quantitative coronary atherosclerosis imaging.**

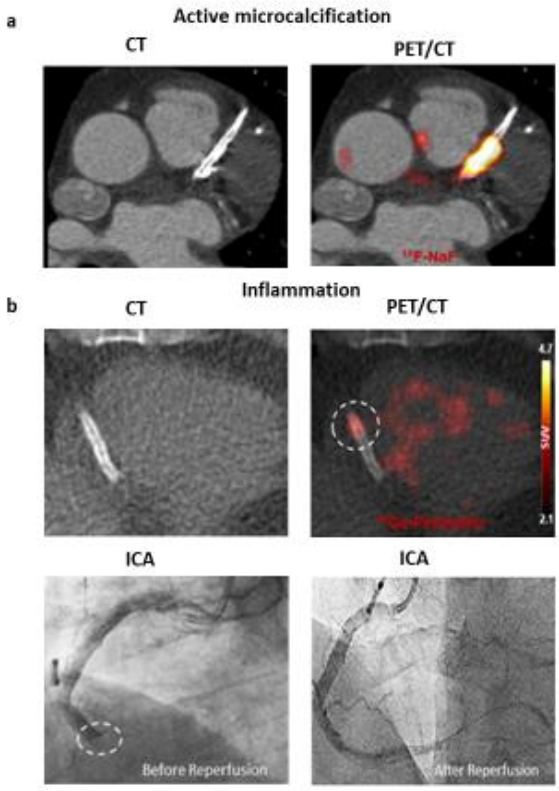

a | Demonstration of active microcalcification using 18F-sodium fluoride (NaF) PET. Example images from the PREFFIRtrial[125] showing active microcalcification in culprit, stented plaque in left anterior descending (LAD) artery. The CT image (left panel) shows the stent in the LAD without a visible abnormality, while the PET/CT (right panel) image shows a focal site of increased active mineral deposition (**FIG. 2**). **b** | Detection of CXCR4-positive inflammatory cells. Computed tomography (CT) (top left panel) and fused CXCR4-targeted PET/CT (top right panel) of culprit stented lesion in acute ST-segment elevation myocardial infarction. Elevated CXCR4 signal (top right panel, dotted circle) representing CXCR4+ inflammatory cell infiltrate[129] can be seen; the corresponding ICA shows the culprit lesion before reperfusion (bottom left panel, dotted circle) and after reperfusion (bottom right panel).

Fig. 8 | **Representative example of coronary radial wall strain analysis.**

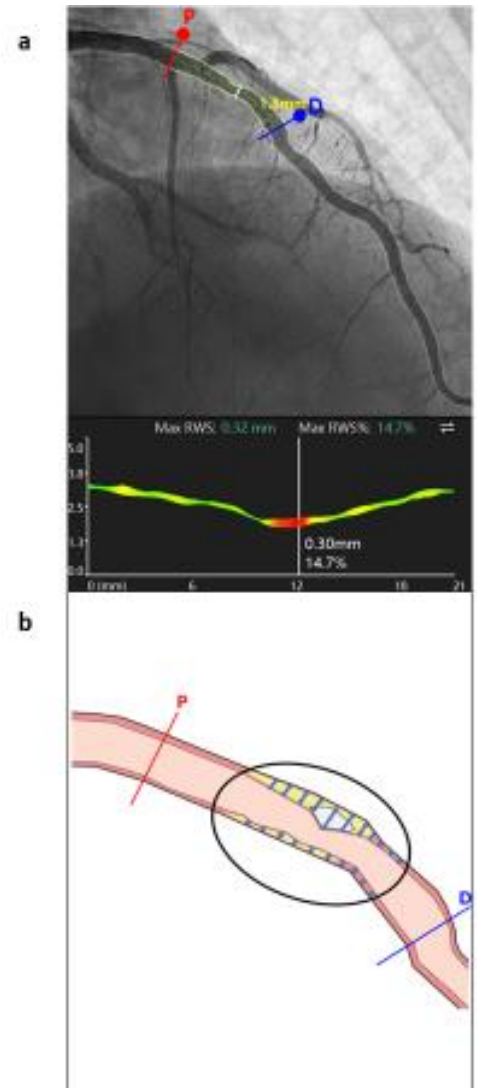

a | Invasive coronary angiography (ICA) shows a moderate lesion in the left anterior descending coronary artery (LAD) (left panel). The white line indicates the region with the highest radial wall strain (RWS) over the cardiac cycle. RWS is estimated using a single ICA projection with minimal lesion overlap and vessel foreshortening. To calculate the RWS, first the lumen diameter change (LDC) along the target vessel is estimated during 4 representative phases of the cardiac cycle (end-diastole, early-systole, end-systole, and end-diastole); the LDC is then computed as the maximal diameter minus the minimal diameter over the cardiac cycle. The RWS is the LDC divided by the maximal diameter. A maximum RWS >12% was suggested as the threshold for defining vulnerable plaque on coronary radial wall strain analysis [130]. In the example shown, RWS derived from ICA images correlated with invasive imaging-derived characteristics of plaque vulnerability such as the presence of thin-cap fibroatheroma. **b** | RWS for the assessment of atherosclerosis (right panel). RWS is the direct reflection of the interplay between the pulsatile coronary blood pressure and the composition of the vessel wall. A higher deformation of the vessel wall (blue two-sided arrows) during the cardiac cycle corresponds to high-strain spots; notice that the most atherosclerotic segments (black circle) have a higher RWS. Vulnerable plaques tend to have higher RWS values and are more susceptible to rupture because of their higher biomechanical stress.
D: distal; P: proximal.

Fig. 9 | **IVUS for quantitative coronary atherosclerosis imaging.**

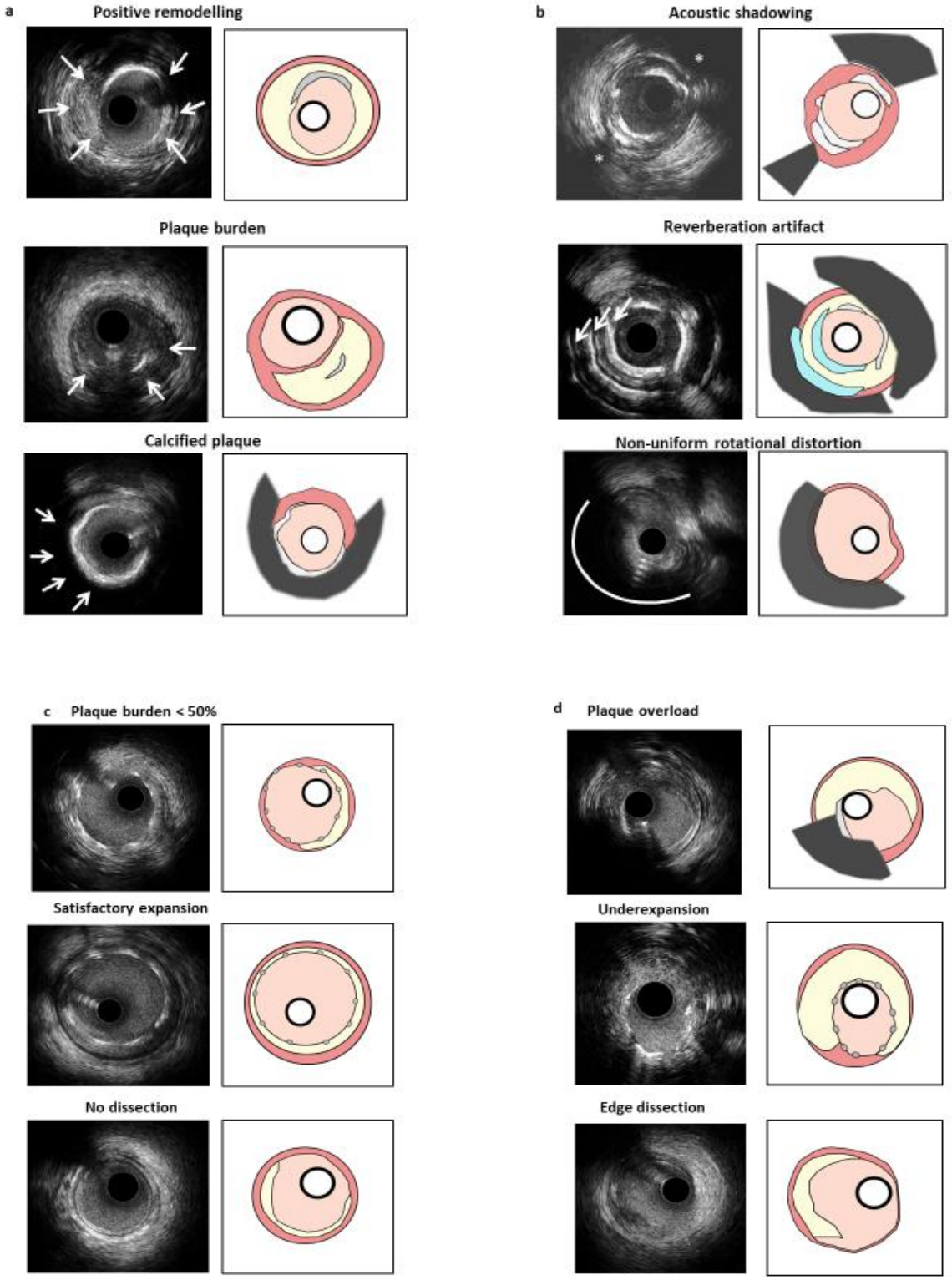

a | IVUS plaque detection and quantification. The panels on the right of the IVUS cross-sectional images are graphic representations of the vessel components and coloured as following: lumen = light pink, vessel wall = dark pink, non-calcified plaque = yellow, calcified plaque = light grey; brown: lipid-rich plaques; red: thrombus; grey circles: stent struts; dark grey= acoustic shadow; blue: reverberation. Positive remodelling (middle-top panel) is the thickening of the vessel wall secondary to coronary plaques (**FIG. 2**); in this example, the thickened wall (arrows) has already narrowed the vessel lumen (top panel). The plaque burden is calculated as the ratio of the atheroma area to the vessel's external elastic lamina (EEL) (arrows);

the atheroma area is calculated by the difference between EEL area and the lumen area (middle panel). Calcified plaque (bottom panel) (arrows) causes acoustic shadowing obscuring the external layers of the vessel wall. **b** | IVUS artefacts. Differentiating artefacts from true structures in IVUS is pivotal for plaque assessment. Acoustic shadowing behind calcific plaque (asterisk) (top panel). Reverberation artefact seen as multiple equidistant reflections from calcium (arrows) (middle panel). Non-uniform rotational distortion is seen from 7 to 12 o'clock (curved dotted arrow) (bottom panel). **c** | Optimal stent implantation by IVUS guidance. For an optimal stent implantation (**FIG. 2**), the following criteria must be met: a plaque burden <50 % at 5 mm proximal or distal to the plaque edge (top panel), stent expansion at the minimal lumen area (MLA) must be > 5.0 mm^2 or 90% of the MLA of the reference segments (middle panel), and no dissection > 3 mm involving the media[136] (bottom panel). **d** | Criteria for stent failure are plaque overload > 50% (top panel), underexpansion (middle panel), and edge dissection (bottom panel).

Fig. 10 | **OCT for quantitative coronary atherosclerosis imaging.**

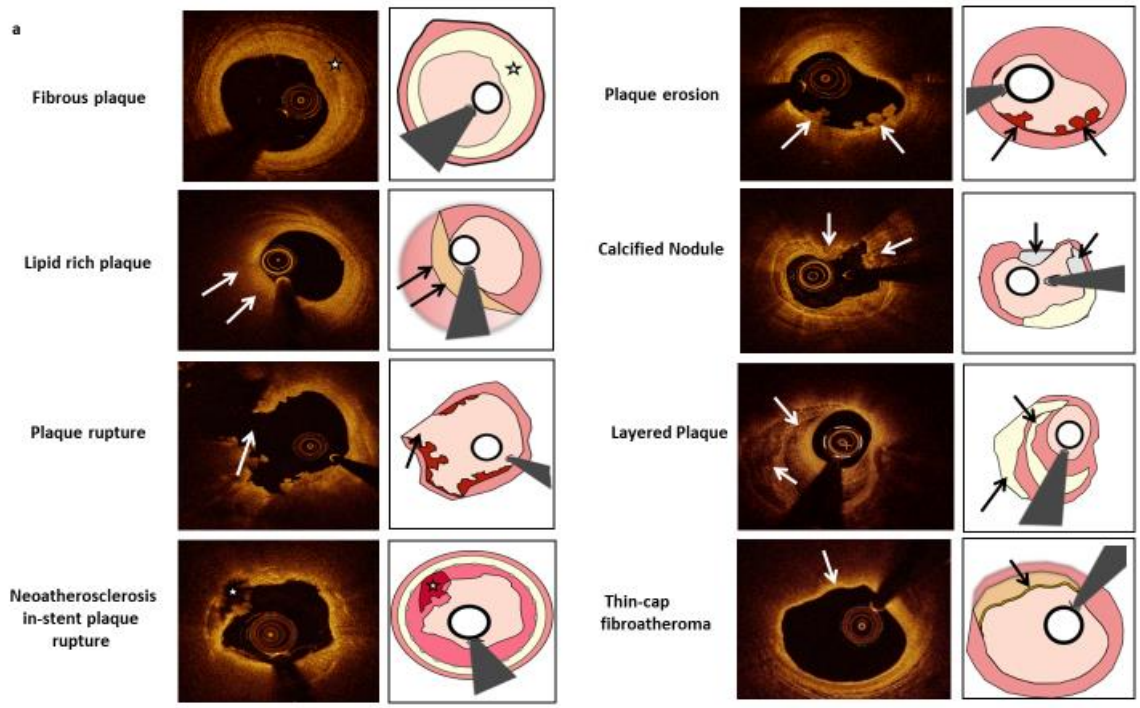

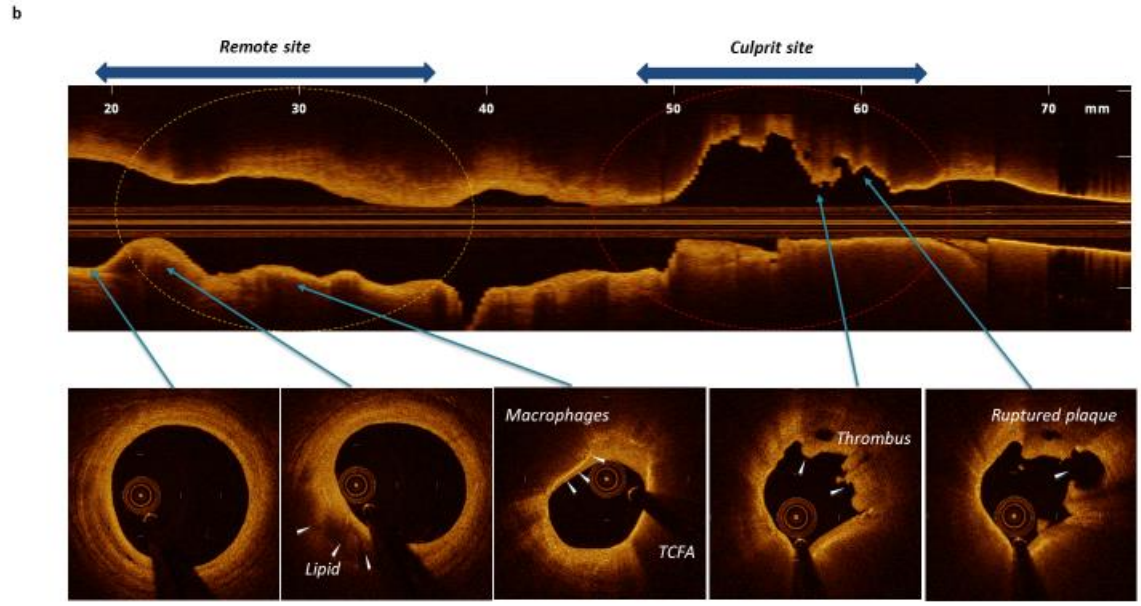

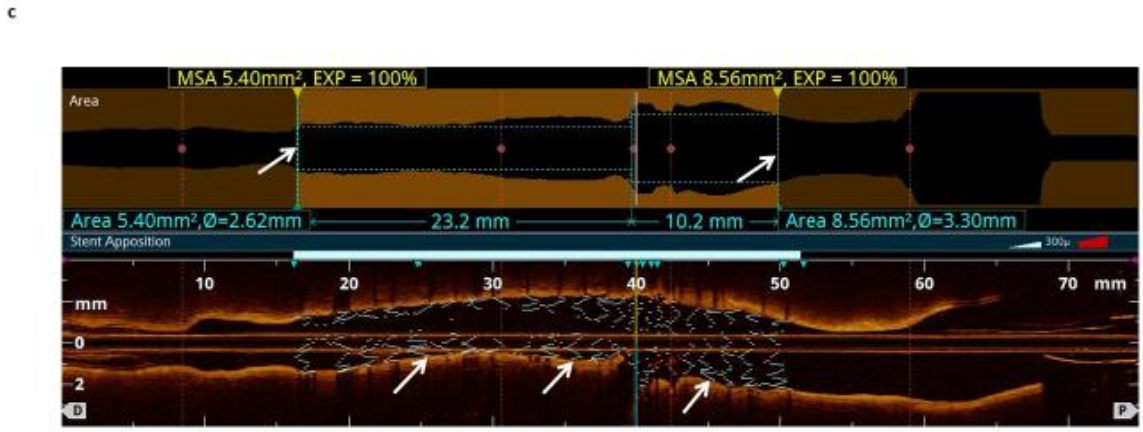

a | Vulnerable plaque features identified by OCT. The panels on the right of the OCT cross-sectional images are graphic representations of the vessel components and coloured as follows: lumen = light pink, vessel wall = dark pink, non-calcified plaque = yellow, calcified plaques = light grey; brown: lipid-rich plaques; red: thrombus; dark grey=shadow produced by the guide-wire. Fibrous plaque: homogeneous signal-rich backscattering regions (asterisk) (top left panel). Lipid-rich plaque: low-intensity regions with diffuse borders and high-intensity overlying bands (middle-top left panel). Plaque rupture: fibrous cap discontinuity and cavity formation within the plaque (middle bottom left panel) (**FIG. 2**). Neoatherosclerosis in-stent plaque rupture: low-intensity region with diffuse borders and within the stent (bottom left panel). Plaque erosion: presence of attached thrombus overlying a visually intact plaque (top right panel). Calcified nodule: one or more regions of calcium protruding into the lumen (middle-top right panel). Layered plaque: plaque with layers of different optical densities (middle-bottom right panel). Thin-cap fibroatheroma (TCFA): plaque with lipid-rich content and a fibrous cap < 65-70 μm (bottom right panel). **b** | Longitudinal view showing different plaque components (lipid-rich, macrophages, TCFA, thrombus and ruptured plaque) along the left coronary artery. Macrophages are seen as a high-intensity confluent region with a signal intensity exceeding that of background noise (middle panel). Thrombus (**FIG. 2**) is seen as a high-intensity backscattering mass protruding into the lumen (middle-right panel). **c** | Stent implantation and automated stent expansion (top panel) with dual segmentation at the left anterior descending artery (LAD) upstream and downstream of the first diagonal side branch (D1); optimal expansion (100% for both segments, blue arrows) and large lumen area (> 4.5 mm^2) were achieved. OCT longitudinal view with stent (bottom) confirming proper expansion (blue arrows) of the stent without strut malapposition inside the LAD.